Wang, H., Xu, Y., Kumar, A., Knorr, K.-H., Zhao, X., Perez, J., Sun, G., Yu, Z.-G. (2023): Temperature and organic carbon quality control the anaerobic carbon mineralization in peat profiles via modulating microbes: A case study of Changbai Mountain. - Environmental Research, 237, Pt. 1, 116904.

https://doi.org/10.1016/j.envres.2023.116904

Temperature and organic carbon quality control the anaerobic carbon mineralization in peat profiles via modulating microbes: A case study of Changbai Mountain

Hongyan Wang[1,2,3], Yijie Xu[1], Amit Kumar[1], Klaus-Holger Knorr[4], Xiaoning Zhao[5], Jeffrey Paulo H. Perez[6], Guoxin Sun[3], Zhi-Guo Yu[1*]

[1]School of Hydrology and Water Resources, Nanjing University of Information Science and Technology, Nanjing 210044, China

[2]Key Laboratory of Watershed Earth Surface Processes and Ecological Security, Zhejiang Normal University, Jinhua, 321004, China

[3]State Key Lab of Urban and Regional Ecology, Research Center for Eco-Environmental Sciences, Chinese Academy of Sciences, Beijing 100085, China

[4]University of Münster, Institute for Landscape Ecology, Ecohydrology and Biogeochemistry Group, Heisenbergstr. 2, Münster 48149, Germany

[5]School of Geographical Sciences, Nanjing University of Information Science and Technology, Nanjing 210044, China

[6]Sec. 3.2 Organic Geochemistry, GFZ German Research Centre for Geosciences, Telegrafenberg, 14473 Potsdam, Germany

*: Corresponding author: zhiguo.yu@nuist.edu.cn

Abstract

Peatlands account for a significant fraction of the global carbon stock. However, the complex interplay of abiotic and biotic factors governing anaerobic carbon mineralization in response to warming remains unclear. In this study, peat sediments were collected from a typical northern peatland-Changbai Mountain to investigate the behavior and mechanism of anaerobic carbon mineralization in response to depth (0-200 cm) and temperature (5°C, 15°C and 20°C), by integrating geochemical and microbial analysis. Several indices including humification indexes (HI), aromaticity, and water extractable organic carbon (WEOC) components were applied to evaluate carbon quality, while 16S rRNA sequencing was used to measure microbial composition. Regardless of temperature, degradations of carbon quality and associated reduction in microbial abundance as well as diversity resulted in a decrease in anaerobic carbon mineralization (both CO_2 and CH_4) towards greater depth. Warming either from 5°C to 15°C or 20°C significantly increased anaerobic carbon mineralization in all depth profiles by improving carbon availability. Enhanced carbon availabilities were mediated by the change in microbial composition ($p < 0.01$) and an increase in metabolic activities, which was particularly evident in the enhanced β-glucosidase activity and microbial collaborations. A remarkable increase of over 10-fold in the relative abundance of the *Geothrix* genus was observed under warming. Overall, warming resulted in an enhanced contribution of CH_4 emission and a higher ratio of hydrogenotrophic methanogenesis, as evidenced by carbon isotope fractionation factors. In addition, deep peat soils (> 100 cm) with recalcitrant carbon demonstrated greater

temperature sensitivity (Q_{10}: ~2.0) than shallow peat soils (Q_{10}:~1.2) when temperature increased from 15°C to 20°C. The findings of this study have significantly deepened our understanding for mechanisms of carbon quality and microbe-driven anaerobic carbon mineralization in peatlands under global warming.

Keywords: temperature, peat profiles; microbe; carbon quality; anaerobic carbon mineralization

1. Introduction

Peatlands account for more than 20% of global carbon storage (~650 Gt) (Harenda et al., 2018; Yu et al., 2010), therefore playing a crucial role in the global carbon cycle and climate change mitigation (Limpens et al., 2008; Leifeld and Menichetti, 2018). As peatland frequently experiences anaerobic conditions (Sihi et al., 2018), organic carbon (OC) decomposition in peat soils is hampered due to oxygen depletion, resulting in massive OC burial in these environments. Recent evidences suggest that soil mineralization converts large organic polymers into monomers, and ultimately back into the atmosphere thereby enhancing global warming (Chen et al., 2023; Davidson and Janssens, 2006; Zosso et al., 2023), leading to positive feedback on climate change. However, in response to warming, the interactions between abiotic and biotic processes governing anaerobic carbon mineralization in peat soils are less studied and remain unclear (Davidson and Janssens, 2006; Wilson et al., 2016; Hopple et al., 2020), this research gap further renders our effort to integrate peatlands into climate earth models. Given ongoing global warming and climate change projections, the role of peatland carbon mineralization in response to warming has garnered considerable research attention. Labile carbon is gradually consumed, and recalcitrant carbon such as humic-like fluorescent components, and aromatic components are preserved in deep peat as burial time progresses (Wang et al., 2021).

Notably, aerobic decompositions of recalcitrant carbon in deep peat are more strongly affected by temperature rise than labile carbon (Hilasvuori et al., 2013; Li et al., 2021; Liu et al., 2016), favoring “carbon quality-temperature” hypothesis (Bosatta and Ågren,

1999). However, the response of anaerobic peat mineralization to global temperature rise, particularly deep recalcitrant carbon, is still poorly studied and a hot topic of scientific debate (Zosso et al., 2023). Wilson et al., (2016) demonstrate that while surface peat decompositions are vulnerable to *in situ* warming, deep peat with recalcitrant carbon is not. However, results from prolonged warming research indicate that carbon in deep peat can also play a large role in carbon oxide (CO_2) and methane (CH_4) emissions under the same conditions mentioned above (Hopple et al., 2020). Field warming is difficult to control and the physiochemical changes in soils are difficult to monitor. For example, whole-system warming might also influence soil moisture content and plant litter input, therefore masking temperature influences (Hu et al., 2019; Hopple et al., 2020). Sihi et al., (2016) conducted a laboratory warming experiment with subtropical peat and found that subsurface peat with recalcitrant carbon is more temperature sensitive, whereas Liu et al., (2019) suggested that surface peat with labile carbon is more temperature sensitive. Given the limited and contradictory findings, there is a need for a comprehensive study to further investigate the warming effect on anaerobic carbon mineralization across the entire depth profiles of peatlands.

Anaerobic carbon mineralization involves enzymatic cleavage of polymers, hydrolysis and fermentation, anaerobic respirations or methanogenesis, and finally the production of CO_2 and CH_4 (Bridgham et al., 2013; Ming et al., 2021). Organic carbon oxidation coupled with the reduction of electron acceptors including nitrate (NO_3^-), manganese (Mn), iron (Fe), sulfate (SO_4^{2-}) and humic substances, contributes to the majority of the

CO_2 emissions from the peatlands, often outperforming methanogenesis. However, as a result of ombrotrophic states, most boreal peatlands emit a significant amount of CH_4, which has a 28-fold stronger global warming potential than CO_2 on a 100-year timescale (Frankenberg et al., 2005). Growing studies indicate that geochemical variables such as water content, nutrient states, organic carbon availabilities and labilities all influence anaerobic organic carbon mineralization and its response to temperature (Ali et al., 2018; Chow et al., 2006). According to Song et al., (2018), labile carbon is the primary driver for microbial mineralization in peat soils. However, it has also been demonstrated that microbial processes play a significant role in OC mineralization (Baldrian et al., 2012; Auffret et al., 2016). Temperature rises may have an impact on key microbial processes in the peat, such as enzymatic activities, microbial abundance and structures (Bragazza et al., 2013; Zhou et al., 2016; Alster et al., 2020), which will, in turn, have an impact on the anaerobic carbon mineralization. For example, microbial community structures and functions in the peat with recalcitrant carbons differ from shallow peat abundant with labile carbons (Lin et al., 2012; Kluber et al., 2020), therefore peat soil at different depth may respond differently to temperature change by interacting with the substrate. Furthermore, warming may alter anaerobic carbon mineralization pathways, because anaerobic respirators and methanogens may adapt differently to changing thermodynamic conditions (Schmidt et al., 2015). A Few studies argue that methanogenesis is more temperature sensitive than CO_2 production (Gill et al., 2017; Sihi et al., 2018; Hopple et al., 2020). Overall, abiotic and biotic factors limit anaerobic carbon mineralization and pathways in response to temperature

rise (Briones et al., 2014; Kumar et al., 2023). There have been few studies that attempt to integrate abiotic factors, particularly carbon qualities coupled, with microbial processes, in order to understand mechanisms of anaerobic carbon mineralization and its response to warming in the whole vertical peat profiles (Li et al., 2021).

The Changbai peatland is a typical boreal peatland in the northeast of China (Zhang et al., 2021). The physiochemical properties of peat are assumed to vary greatly in vertical peat profiles, with more recalcitrant carbon found in deep peat (Lamit et al., 2021; Tfaily et al., 2014), allowing us to investigate how biotic processes interact with peat substrate to control anaerobic organic carbon mineralization, particularly in response to temperature rise. This study integrate geochemical analysis and microbial sequencing to (i) identify the mechanisms of interaction between peat substrate and microbial processes on controlling CO_2 and CH_4 emissions in vertical peat profiles, (ii) demonstrate temperature (5°C, 15°C and 20°C) influences for anaerobic carbon mineralization in peat profiles as related pathways, and (iii) elucidate mechanisms of anaerobic carbon mineralization in response to temperature rise.

2. Materials and methods

2.1 Study area and sample collections

Ombrotrophic peatlands, a typical boreal peats, are widely distributed in the Changbai Mountain with an area of up to 314 km^2 and carbon storage of around 94 Tg (Gao et al., 2016). The Dongtu peatland (42°16.249N, 127°51.665E) is located within "CBM Biosphere Reserve" in the western part of Changbai Mountain (**Fig. S1**). The peatland developed around 2000 years ago with a depth of around 2.0 m, which is similar to

most boreal peatlands (Loisel et al., 2014). It belongs to the temperate continental climate, with annual precipitation varying from 700 to 1400 mm (Bao et al., 2010a). Average annual temperature in Changbai Mountain is around 5°C, and the ground temperature in the growing season could increase to 20°C (Zhang et al., 2021). It is water-logged mostly throughout the year. Plant species developed in the peatland mainly include *Trichophorum sp.*, *Carex sp.*, and *Oxycoccus palustris*.

In the field campaign, six peat cores were collected within an area around ~15m × ~15m, using a Russian peat corer in the hollow area of Dongtu peatland, the peat core was separated on-site into 10-cm deep sections. Each section was wrapped with sterilized aluminum foil, and put into sterilized bags flushed with N_2 gas. Soil samples were frozen (-20°C) upon arrival in the laboratory, and stored until the experiment was conducted. Prior to incubation experiments, peat cores were thoroughly mixed according to depths (0-10 cm, 10-20 cm, 30-50 cm, 50-70 cm, 80-100 cm, 120-150 cm, and 170-200 cm). After taken out visible plant debris, subsamples were freeze-dried for the determination of chemical properties, and remaining soils were stored at 4°C for 2-3 days before the incubation experiment.

2.2 Analysis of physiochemical properties in initial peat

Carbon (C) and nitrogen (N) content in initial peat layers were measured by an elemental analyzer (UNICUBE, Germany). Iron oxides and iron oxides-bound organic carbon content were analyzed using dithionite-citrate-bicarbonate (DCB) extraction methods (Coward et al., 2017; Wang et al., 2020). After two cycles of repeated extraction, slurries were washed with 20 mL 0.05 mol/L HCl. All extracts were

158 collected for measuring dissolved organic carbon (DOC) and iron (Fe) concentrations.
159 The DOC concentration was analyzed on a TOC analyzer (TOC-L, Shimadzu, Japan),
160 while the Fe concentration was analyzed spectrophotometrically by ferrozine methods
161 (Viollier et al., 2000; Khan and Tian, 2018).
162 The FTIR spectra (Bruker, Optik) of peat samples were previously measured using an
163 analytical method described in Broder et al., (2012), analysis was recorded from 400
164 cm^{-1} to 4000 cm^{-1} with a resolution of 1 cm^{-1} (**Fig. S2**). The adsorption band at ~1090
165 cm^{-1} is attributed to -OH vibrations of polysaccharides, while adsorption band at ~1630
166 cm^{-1} is characterized by aromatic components such as lignin (Niemeyer et al., 1992),
167 therefore the ratio of ~1630 cm^{-1}/1090 cm^{-1} is indicative of humification index (HI)
168 (Cong et al., 2023; Niemeyer et al., 1992). The HI of peat samples used in the
169 experiment was averaged using peat included in corresponding depths.
170 The water-extractable organic carbon (WEOC) was extracted by shaking freeze-dried
171 peat in ultrapure water at a solid-to-liquid ratio of 1:10 (w:v) for 12h. Following by
172 suspension filtered through 0.45-μm Nylon filters, supernatant was acidified to pH < 2
173 using H_3PO_4, and concentrations of WEOC were analyzed by a TOC analyzer (TOC-L,
174 Shimadzu, Japan). An ultraviolet and visible spectrometer (DR6000, Hach) was used
175 to measure the UV absorbance of supernatants. Specific UV absorbance at 254 nm
176 ($SUVA_{254}$) was calculated as ultraviolet absorbance at 254 nm divided by DOC
177 concentrations, to indicate the aromaticity of WEOC (Weishaar et al., 2003). To further
178 characterize the WEOC, three-dimensional fluorescence excitation emission matrices
179 (EEMs) were obtained on a fluorescence spectrophotometer (Cary Eclipse) with an

excitation range of 200-450 nm and emission range of 200-600 nm, respectively.

2.3 Microcosm experiment

Microcosm experiments were prepared in the glovebox. The 10 g of wet peat (~ 2 g in dry weight) was placed into 250 mL serum bottles, and 100 mL of deoxygenated ultrapure water was supplemented. Serum bottles were sealed using 2 cm-thick butyl stoppers (Glasgerätebau Ochs, Bovenden, Germany), and crimped with aluminum caps. Thereafter, serum bottles were N_2 purged for 30 minutes. Peat layers from 7 depths were incubated at temperatures of 5°C, 15°C and 20°C in triplicates, totally 63 samples.

2.4 Gas sampling and measurements

In this experiment, total 7 gas sampling events were conducted, respectively at 10, 15, 22, 33, 44, 55, and 63 days. The 2-3 mL gas inside serum bottles was sampled by a syringe, which was N_2 purged before use. Then samples were injected into vacuumed serum bottles. Gas concentrations were measured by gas chromatography (GC system, Agilent, 8090B, USA). The cumulative carbon mineralization (CCM) content produced was averaged to dry peat soils per gram.

Carbon isotopes ($\delta^{13}C$) in CH_4 and CO_2 were analyzed by an isotope ratio MS (delta V advantages, thermos, Germany), and results were reported as $\delta^{13}C$ of CH_4 or CO_2 ($\delta^{13}C_{CH4}$ or $\delta^{13}C_{CO2}$), which value was standardized by VPDB. Resulting from extreme low CH_4 emissions at 5°C, the $\delta^{13}C$ of CH_4 was unable to measure. Fractionation factor (α_c) was calculated by $\delta^{13}C_{CH4}$ or $\delta^{13}C_{CO2}$ (Conrad, 2005):

$$\alpha_c = (\delta^{13}C_{CO2} + 10^3) / (\delta^{13}C_{CH4} + 10^3)$$

2.5 Water chemistry and microbial property analysis

The DOC concentrations in microcosm samples were monitored, and properties were also analyzed by EEMs with the protocols described above. Low molecular weight organic acids (LMWOA) were also analyzed in selective water samples of 15°C and 20°C by high-performance liquid chromatography (HPLC) (SPD–M20A, Shimadzu). Following incubations, peat samples were destructively sampled for enzymatic and 16S rRNA sequence analysis. Each sample was assayed for enzymatic activities, activities of β-glucosidase (BG), leucine-amino peptidase (LAP), and acid phospho-monoesterase (PHOS) were respectively indicated as representatives of C, N and P cycling (Steinweg et al., 2018a). Enzyme assays were referred to Jackson et al., (2013) and AminiTabrizi et al., (2022). To prepare soil slurries, a 50 mM acetate buffer was used, and for each sample, a set of solutions was prepared both with and without the enzyme substrates, namely p-nitrophenol. Absorbance of solutions was measured at 410 nm. For the LAP enzyme activity, L-leucine-7-amido-4-methylcoumarin hydrochloride was used as the substrate, fluorescence was measured on a BioTek Microplate reader with excitation at 365 nm and emission at 450 nm, respectively.

Microbial DNA from each peat sample was extracted with FASTDNA Spin Kit (MP Biomedicals, Solon, OH). Following the purification, DNA extracts were quantified using NanoDrop spectrophotometer (Nanodrop Inc., Wilmington, DE, USA). The V4 region of 16S rRNA gene was amplified with primer set 515F (5'-GTGCCAGCMGCCGCGG-3') and 806R (5'- GGACTACHVGGGTWTCTAAT-3'), details about PCR reactions and thermal programs were shown in **Table S1**. Obtained amplicons from PCR reactions were sequenced in the Illumina Miseq platform of

Biozeron (Shanghai).

Raw sequencing data were demultiplexed and filtered using in-house perl scripts. Specifically, reads with an average quality score of less than 20 over a 10 bp sliding window were trimmed off, and truncated reads short than 50 bp were discarded. Furthermore, reads with barcode mismatching or containing ambiguous characters were removed. Only sequences having overlaps longer than 10 bp were assembled. Assembled reads were clustered into OTUs with a 97% similarity cutoff using UPARSE (version 7.1 http://drive5.com/uparse/), and chimeric sequences were identified and removed using UCHIME. Finally, each OTU was classified with silva (SSU138.1) 16S rRNA database using a confidence threshold of 80%. Raw 16S rRNA sequences are available in the National Center for Biotechnology Information (NCBI) Sequence Read Archive under the accession number PRJNA967048.

2.6 Statistical analysis

2.6.1 The Q_{10} estimation

The Q_{10} value was used to indicate temperature sensitivity of anaerobic peat mineralization. The Q_{10} of cumulative carbon mineralization (μg CO_2+CH_4-C g^{-1} dry peat) was calculated as (Mao et al., 2022):

$$Q_{10} = (R_h/R_l)^{10/(Th-Tl)}$$

Where R_h and R_l stand for CCM (sum of C-CO_2 and C-CH_4) under high (T_h) and low (T_l) temperature, respectively.

2.6.2 PARAFAC analysis

The parallel factor (PARAFAC) analysis was applied to identify specific complexes presenting in DOM fluorophores (Stedmon et al., 2003; Stedmon and Markager, 2005). In this study, total 190 water samples with excitation wavelengths and emission wavelengths ranging from 200 to 500 nm were included in datasets. The analysis was conducted in the MATLAB with DOMFluor toolbox. In the result, a three-component model can best explain data sets, including terrestrial humic-like component (C1), tryptophan-like components (C2, also called protein-like component), and humic-like substance, but with reduced quinone-like characteristics (C3) (**Fig. S3**; **Table S2**). The relative abundance of each component was calculated as ratio of its fluorescence intensity to sum of fluorescence intensities from all components.

2.6.3 Statistical analysis

The Pearson correlation was applied to show relationships between CCM and geochemical parameters or microbial properties, which was conducted in SPSS statistics 26.0. Furthermore, the SPSS software was used to conduct one-way analysis of variance (ANOVA).

To analyze influences of temperature on microbial compositions, the Bray-Curtis distance was calculated in the R package "vegan", the significance level was further analyzed by multivariate analysis of variance (PERMANOVA). Moreover, co-occurrence networks were created to visualize interactions between microbes, correlations were built using Spearman correlations with R^2 greater than 0.7. Network characters including nodes, edges and modularity were calculated in the R package "Hmisc" and "Igraph" (Harrell, 2009; Csardi and Nepusz, 2006). Finally, the network

was visualized by “Gephi”. Node degrees, referring to connections (edges) that each node has with other nodes in the network, was used to show microbial collaborations (Lü et al., 2022).

For elucidating linkages between abiotic and biotic factors under warming and their contributions to CCM, structural equation modelling (SEM) was applied for peat soils in vertical profiles using AMOS software (AMOS 17.0.2, student version). The SEM’s goodness-of-fit was evaluated by comparative fit index (CFI), P-value, Chi-square (χ^2), and AIC value.

3. Result

3.1 Geochemical properties of pristine peat samples

Geochemical properties of vertical peat profiles were shown in **Table 1**. The C/N ratio demonstrated a narrow range (18.90 ~ 21.00), except a slightly lower value in surface peat (15.71). Iron oxides content generally decreased from 1.85% in surface peat to ~0.58% in bottom peat, while Fe oxides-extractable organic carbon was invariant through depth profiles, except for slightly higher content (1.67 g kg^{-1}) in surface sediments. The OC quality exhibited a general decline towards greater depth, as evidenced by various indices (**Table 1**). The HI increased from 0.71 to 0.95 towards greater depths, except that the basal layer in the bottom had a lower HI (0.35). Furthermore, aromaticity of WEOC as $SUVA_{254}$ also indicated vertical distribution patterns, increasing from 1.76 L mg C^{-1} m^{-1} in the surface peat to 5.19 L mg C^{-1} m^{-1} in the bottom peat. The protein-like organic carbon (C2) in the WEOC identified by PARAFAC declined from 48% in the surface peat to 20.3% in the bottom peat.

3.2 CO_2 and CH_4 emissions in vertical peat

Both cumulative emissions of CO_2 and CH_4 generally decreased with depth, except that peat samples had low CH_4 emissions under 5°C and did not show significant differentiation (**Fig. 1**). Noticeably, peat samples from 30–50 cm indicated deviations from declined patterns with depth, as evidenced their notably low cumulative CO_2 and CH_4 emissions (**Fig. 1**). The CO_2 emission accounted for 99.60% to 99.98% of CCM (**Table 2**). Furthermore, under variable temperatures, anaerobic carbon decompositions (sum of DOC, CO_2 and CH_4) did not indicate vertical patterns except for slightly higher decomposed content at surface peat (**Table S3**).

Overall, temperature rises either from 5°C to 15°C or from 15°C to 20°C significantly enhanced CH_4 emissions ($p < 0.05$), while CO_2 emissions remarkably increased from 5°C to 15°C or 20°C ($p < 0.05$) (**Fig. 1 and Table 2**). The CCM content was averaged at 0.25 mg g^{-1} dry peat at 5°C, however, it was averagely 2.2 and 2.6 times higher at 15°C and 20°C. Noticeably, contribution of CH_4 emissions to CCM enhanced from average of 0.03% at 5°C to 0.09% at 15°C and 0.20% at 20°C, respectively. Both Q_{10} at 15-5°C ($Q_{1015\text{-}5°C}$) and 20-15°C ($Q_{1020\text{-}15°C}$) did not vary consistently with depth, ranging from 1.77 to 2.56, and from 0.96 to 2.14, respectively (**Table 2**). Under 5°C to 15°C, deep peat (> 100 cm) had slightly lower Q_{10} (~ 1.7) than shallow peat (~2.0). Under 15°C to 20°C, deep peat together with peat sediments from 30–50 cm indicated significantly higher temperature sensitivity (~2.0) than shallow peat sediments (~1.2) (**Table 2**).

At 15°C and 20°C, the $\delta^{13}C$ signature ranged from -25.5‰ to -22.7‰ in CO_2 and from

-63.8‰ to -41.5‰ in CH_4, respectively, which both generally increased with depth (**Fig. 2**). The fractionation ratio of CO_2 and CH_4, represented by α_C [($\delta^{13}C$- CO_2 + 1000) / ($\delta^{13}C$- CH_4 + 1000)] varied between 1.016 to 1.044. The $\delta^{13}C$ isotope in both CO_2 and CH_4 generally increased with depth, except that exponentially higher value was found at a depth of 30-50 cm. Under warming, most peat samples had a significant decrease in $\delta^{13}C$-CH_4, accompanied by a general increase in α_C.

3.3 DOC concentration and characteristics through incubation stage

The concentration of dissolved organic carbon (DOC) in each microcosm did not exhibit significant changes throughout the entire incubation stage, however, there was a tendency for the DOC concentration to increase with depth (**Fig. 3a**). At 5°C, surface peat had the DOC concentration averaged at ~9 mg L^{-1} of entire incubation stage, and increased to ~14 mg L^{-1} at the bottom peat, whereas warming increased DOC concentration throughout peat profiles in general (**Fig. 3a**). Furthermore, relative contribution of protein-like components to DOC pool was rapidly declined through the incubation period, while the relative ratio of reduced quinone-like organic carbon enhanced (**Fig. S4**). Except for propionate (0.14 to 0.24 mg L-1), other LMWOA such as acetate, and lactate were not detected in the majority of the water samples (**Fig. S5**). Propionate concentrations tended to increase as a function of depth, and warming slightly decreased its concentrations throughout profiles.

3.4 Enzymatic activities, microbial compositions in vertical peat profiles

Enzymatic activities encoding C, N, and P cycles indicated no depth differentiation, while temperature rise significantly enhanced BG enzyme activity across depth profiles

(**Fig. 3b, Fig. S6**). The activity of BG enzyme was 560 nmol activity g^{-1} dry peat h^{-1} at 5°C on average, while it is around 2.4 and 3.6 times higher at 15°C and 20°C (**Fig. 3b**). The relative abundance and diversity of microbe in each microcosm were indicated as Chao1 index and Shannon diversity, respectively (**Fig. S7**). Irrespective of temperature, relative abundance and community diversity of microbes generally decreased with depth, declining from 705.8 and 5.68 at the surface sediment to 433.3 and 4.67 at the bottom sediment, respectively. However, the peat sediment from 30-50 cm presented slightly lower microbial relative abundance and diversity than nearby sediments.

Main bacterial phylum detected in peat samples include *Proteobacteria* (41.5%-60.6%) and *Acidobacteria* (2.58%-24.1%) (**Fig. 4A**). At the family level, the relative abundance of *Syntrophaceae* (around 0.6%), which is one of the dominant bacteria in the peat profile, was also decreased towards greater depth (**Fig. 5e**). Even though both acetoclastic and hydrogenotrophic methanogens were detected in the peat sediments, however, the acetoclastic *Methanotrichaceae* (formerly *Methanosaetaceae*) and *methanosarcinaceae* were shown as the main family (**Fig. S8**).

The principal coordinate analysis (PCoA) suggested that the first two PCoA axis could explain 55% of variances in microbial compositions (**Fig. 4B**). Increase in temperature from 5°C to 15°C or 20°C significantly changed microbial community compositions ($p < 0.01$). Noticeably, warming greatly enhanced the relative abundance of *Acidobacteria* across peat profiles, with an average relative ratio of 5.3% at 5°C, increasing to more than 16% at 15°C or 20°C (**Fig. 4A**). At 5°C, the genus *Geothrix* only accounted for less than 1% of mean relative abundance, and reached more than 10% at 15°C, or 20°C

(**Fig. 4C**). No significant change was observed in the relative abundance of total methanogens or any specific methanogen under temperature increase.

To further explore the temperature effect on microbial community structures, co-occurrence networks were constructed to present relationships between microbes (**Fig. S9, Fig. 4D**). The network at 15°C and 20°C respectively contained 1.26 times more links and 1.20 times more positive links than 5°C. Furthermore, node degrees of 15°C and 20°C were significantly higher than that at 5°C.

3.5 Integrated abiotic and biotic factors influencing organic carbon mineralization

At low temperature (5°C), CH_4 emissions did not demonstrate significant variations in different depths. Amounts of cumulative CH_4 and CO_2 emissions were statistically related to each other at 15°C or 20°C ($p < 0.05$), respectively (**Fig. S10**). Therefore, they were both proportional to CCM, and factors influencing CCM were also closely related to CH_4 and CO_2 emissions.

Under 20°C, carbon quality proxies including HI, aromaticity and ratio of protein-like components suggested statistical correlations with cumulative carbon mineralization content (**Fig. 5a-c**). The HI and aromaticity negatively correlated to CCM, while ratio of protein-like components positively correlated to CCM. Microbial properties including bacterial abundance (Chao1 index), diversities (Shannon index) and abundance of *Syntrophaceae* were positively correlated to cumulative carbon mineralization (**Fig. 5def**). Temperature rise induced enhancement of CCM was accompanied by significant increases in enzymatic activities and changes in microbial compositions. However, no specific environmental and microbial variables were

correlated with $Q_{1015\text{-}5^{\circ}C}$ and $Q_{1020\text{-}15^{\circ}C}$.

The structural equation model could explain 79% of variations in CCM (**Fig. 6a**). Both carbon quality (indicated by aromaticity) and temperature influenced the CCM by shifting microbial compositions. Carbon quality, temperature and microbial communities were dominant influencing factors for CCM with standardized total effects of 0.62, 0.55 and 0.75, respectively (**Fig. 6b**).

4 Discussion

4.1 Vertical stratifications of organic carbon quality and microbial compositions

Degradations in OC quality are characterized by the loss of labile organic carbon, such as protein-like components, as well as an increase in humification and aromaticity (Broder et al., 2012; Logue et al., 2015; Heslop et al., 2019). It is consistent with previous studies, showing that peat samples are visualized with carbon quality degradations towards deeper peat (Hilasvuori et al., 2013; Li et al., 2021). Terrestrial humic and protein-like components identified by EEM-PARAFAC are widely distributed in terrestrial aquatic systems. However, a large contribution of reduced quinone-like components appears to be unique in the anoxic environment, as identified in other peatlands by Tfaily et al., (2015) and lakes by Cory and McKnight, (2005).

Acidobacteria and *Proteobacteria* predominance in ombrotrophic peatlands are also typical, which could well adapt to an acidic environment (Urbanová and Bárta, 2014; Wilson et al., 2016; Birnbaum et al., 2022). Co-variant carbon quality, microbial abundance, and diversities are consistent with previous microbial studies in peatlands (Lipson et al., 2013, Lin et al., 2014), indicating that the availability of labile carbon

sources limits the growth and diversity of microbial communities. Noticeably, peat extracted at depth of 30-50 cm has lower microbial abundance and diversity compared with underlying or overlying peat, which could be attributed to poor OC quality. Although we do not observe differentiation in other OC quality indexes such as HI, the $\delta^{13}C$ isotope of both produced CO_2 and CH_4 from 30-50 cm is higher than underlying and overlying peat. Carbon isotopic fractionation occurs during SOM decomposition, which leads to ^{12}C enrichment in the released CO_2, while ^{13}C enriched in the residual SOM (Fernandez et al., 2003), therefore the relative enrichment of ^{13}C in CO_2 from 30-50 cm indicates recalcitrant characters of OC (Alewell et al., 2011). vertical patterns of organic carbon quality and co-variant microbial compositions will have an impact on *in-situ* processed biogeochemical cycles, such as CH_4 emissions.

4.2 The depth-dependent anaerobic CO_2 and CH_4 emission is driven by the Interaction of organic carbon quality and microbial compositions

Quinone moieties in humic substances, acting as an electron acceptor, could play a crucial role in respired production of CO_2 (Gao et al., 2019; Guth et al., 2023), as evidenced by the rapid increase of reduced-quinone like humic moieties in our study. However, the relative contribution of reduced-quinone like humic moieties in peat samples is not significantly differentiated. Therefore, depth-dependent anaerobic CO_2 emissions could be related to vertical stratifications of OC liabilities and microbial compositions.

The Depletion of most organic acids in microcosms indicates that syntrophic or respiring microbes consume the LMWOA rapidly. Thus fermentations of high-

molecular weight OC may be rate-limiting for CO_2 production, which may be influenced in part by OC lability (Drake et al., 2015). Previous studies also found rapid LMWOA turnover in peat sediments due to the presence of diverse syntrophic microbes and methanogens (AminiTabrizi et al., 2023). Consistently, DOC concentrations in deep peat are unexpectedly higher than those in shallow peat, which could be attributed to the recalcitrant properties of deep DOC. Furthermore, a lower relative abundance of respiring or syntrophic microbes in deep peat, such as *Syntrophaceae,* could further contribute to a slightly lower turnover of LMOWA, as evidenced by slightly higher propionate concentrations in deep peat samples, therefore contributing to a lower respiring rate.

For the CH_4 productions, the $\delta^{13}C$ isotope in CH_4 and fractionation factor α_c were signatures of acetolactic methanogenesis dominated in peat profiles (Whiticar, 1999), consisting of the predominance of acetoclastic *Methanotrichaceae* and *Methanosarcinaceae*. The decrease in methanogen abundance with depth corresponds to a decrease in CH_4 emissions. Decomposition of organic acids by syntrophic bacteria directly provides substrates (such as acetate) for methanogens (Conard, 2020), and a lack of labile carbons and syntrophic partners could directly result in lower CH_4 production.

Although microbe abundance and diversity may be directly mediated by OC lability. Under field-relevant conditions, thermodynamic limitations such as end product accumulations (e.g. CO_2 and CH_4) and a lack of diffusive transport could also constrain the abundance of related microbes and activities in deep peat (Beer and Blodau, 2007;

Bonaiuti et al., 2020), which deserved further evaluateion.

4.3 Warming effects for overall anaerobic carbon mineralization

Our results demonstrated that increasing the temperature could increase anaerobic carbon decomposition and subsequent mineralization, which was primarily mediated by biotic mechanisms. The findings of this study partially agree with recent research on the effect of temperature on C cycling, both in laboratory and field-scale studies (Ali et al., 2018; Tong et al., 2021). In this study, we found no evidence of temperature rise-induced microbial diversity loss as previously reported (Yang et al., 2021; AminiTabrizi et al., 2023). Extremely high temperatures used in previous studies might cause microbes to be not well adapted (Fierer et al., 2006).

In this study, we observed a significant shift in the abundance of specific bacteria. Because each taxonomic group contains different species with distinct preferable habitats, they might exhibit different growth rates under specific temperature and substrate conditions, altering OC degradation and pathways. *Acidobacteria*, a typical oligotrophic and K-strategy phylum (Davis et al., 2011; Fierer et al., 2007), has a number of sub-lineages capable of anaerobic OC degradations, especially for recalcitrant carbon in northern peatlands (Dedysh, 2011; Li et al., 2019; Schmidt et al., 2015). *Acidobacteria* could play a more prominent role in recalcitrant carbon fermentations or respirations as temperature rise, the increase in the relative abundance of *Acidobacteria* is partly consistent with a previous study conducted in forest soils, which indicates that K-strategy microbes become more dominant in recalcitrant carbon degradations with temperature rise (Li et al., 2021).

Geothrix, a genus belonging to *Acidobacteria*, responds uniquely to temperature rise and even becomes the most abundant genus at deep peat under 15°C/ 20°C. The *Geothrix sp.* is widely found with high abundance in the northern acidic wetlands (Dedysh, 2011; Pankratov et al., 2008), demonstrating remarkable capabilities of respiring several simple organic acids and long-chain fatty acids with Fe(III) alternatively quinone as electron acceptors (Coates et al., 1999). With enhanced anaerobic respiration under warming, more electrons flow into humic substances, resulting in a decrease in the redox potential of OC. the *Geothrix*, on the other hand, can utilize electron acceptors across a wide range of redox potentials (Mehta-Kolte and Bond, 2012), which could explain the increase in *Geothrix* abundance, and thus contribute to anaerobic respiration., the increase of oligotrophic bacteria, especially *Geothrix*, should be further verified in more peatlands. Under global warming, oligotrophic microbes especially Geothrix might play a significant role in peatland respirations.

Aside from differences in microbial compositions, enhanced microbial activities with temperature rise also contributed to enhanced anaerobic carbon decomposition and mineralization. The BG enzyme is essential for the complete hydrolysis of cellulose into glucose (Steinweg et al., 2018b), and its activity is consistently enhanced throughout the peat profile as temperature rises, prompting cellulose decompositions and providing a respiration source for secondary fermenters such as *Geothrix*. Similarly, increases in OC-hydrolyzing enzyme activities with temperature have previously been reported in several peatlands (Steinweg et al., 2018b; Verbeke et al., 2022), indicating

that the limitation of carbon-hydrolyzing enzyme activities for anaerobic carbon mineralization caused by low temperatures are widely distributed in peatlands.

Furthermore, an increase in node degrees and microbial correlations indicates that microbial collaborations enhance and become more efficient in carbon turnover under higher temperature (Lü et al., 2022), the propionate concentrations consistently decrease as temperature rises.

4.4 Temperature sensitivity of anaerobic carbon mineralization and related pathways

The Q_{10} of CCM ranges from ~1.0 to ~2.5 in the current study, which is comparable to previous studies on peatlands (illustrated in **Table S4**). Taking into account those existing studies, it suggests that Q_{10} of anaerobic carbon mineralization in peatland is site and depth specific, indicating the complex controlling of peat physiochemical properties and microbial properties and deposition histories.

Deep peat (>100 cm) with recalcitrant carbons demonstrated a higher Q_{10} value than shallow peat under higher temperature (15°C-20°C). Consistently, peat sediments from 30-50 cm with more recalcitrant carbon than nearby peat layers had higher Q_{10}. The higher temperature sensitivity of deep peat was consistent with most studies shown in **Table S4**. This result is consistent with aerobic carbon mineralization and supports the "carbon quality-temperature" theory, which states that decomposition of recalcitrant carbon has stronger temperature dependence than labile carbon as it is thermodynamically limited (Bosatta and Ågren, 1999).

The microbial compositions in peat sediment might have an impact on Q_{10}. Under high

temperatures (15-20°C), labile carbon is rapidly consumed, and microbes involved in degrading recalcitrant carbon would take advantage of degrading recalcitrant carbons under thermodynamically favorable conditions, resulting in higher Q_{10}. We discovered that decomposed OC contents of shallow peat and deep peat were similar, indicating that microbes in deep peat specialize in recalcitrant carbon degradations. Another recent study also demonstrated that bacteria that work on recalcitrant OC degradations could increase Q_{10} of anaerobic carbon mineralization (Li et al., 2021). These microbial survival strategies were recently discovered in *in-situ* warming experiments which revealed that deep recalcitrant carbon had higher temperature sensitivities than surface-labile carbons (Chen et al., 2023). In contrast, microbially driven recalcitrant carbon degradations are energy unfavorable under low temperatures (5-15°C), resulting in less temperature sensitivity in deep peat. However, the peat sample from 30-50 cm with recalcitrant carbon is observed to have greater temperature sensitivity under 5-15°C. Such discrepancy might be due to a difference in molecular structures between peat from 30-50 cm and deep peat, which requires further investigation.

Temperature sensitivities of methanogenesis were noticeably higher than CO_2 productions, contributing to an increase in CCM with temperature. This finding is consistent with previous microcosm studies and *in situ* warming experiments (Sihi et al., 2018; Hopple et al., 2020). It suggests that methanogens are more active and efficient in LMWOA than respiring microbes under 15°C and 20°C, as the relative abundance of methanogens did not change significantly in this study. Compared with acetoclastic methanogenesis, hydrogenotrophic methanogenesis is more

thermodynamic favorable (Thauer et al., 2008). As a result, hydrogenotrophic microbes will outcompete acetoclastic methanogens for available substrate being available under rising temperature. a higher contribution of CH_4 to greenhouse gas emissions and altered methanogenesis pathways should be considered in a warming world.

5. Conclusion

Our findings suggest that microbial diversities and abundance are directly modulated by the lability of organic carbon, resulting in a decrease in CO_2 and CH_4 production from anaerobic respiration as depth increases in peatlands. Overall, rising temperature enhances anaerobic carbon mineralization through peat profiles, which is directly linked to enhanced metabolic activities and changes in community compositions. The oligotrophic *Acidobacteria*, particularly the genus *Geothrix*, increased significantly as temperature rose. Noticeably, this study shows that deep peat with recalcitrant carbon may have higher temperature sensitivities under warming conditions. The contribution of CH_4 to anaerobic carbon mineralization is also elevated under higher temperatures, further amplifying warming effects, and creating a positive feedback loop. With ongoing global warming, it is critical to consider the altered carbon mineralization pathways, as well as carbon emissions from deep peat.

Acknowledgement

All analyses except that FTIR analyzing were conducted in NUIST. We acknowledge the help from Dr. Fengwu Zhou for SEM analysis. We further acknowledge the financial support from National Science Foundation of China (Nos. 42207268, 41877337), and Natural Science Foundation of Jiangsu Province (No. SBK

2022044914), as well as Open Fund Project of Key Laboratory of Watershed Surface Process and Ecological Security of Zhejiang Normal University (No. KF-2022-08). JPHP acknowledges the GFZ Discovery Fund for his research fellowship.

References

Alewell, C., Giesler, R., Klaminder, J., Leifeld, J., Rollog, M., 2011. Stable carbon isotopes as indicators for environmental change in palsa peats. Biogeosciences 8, 1769–1778. https://doi.org/10.5194/bg-8-1769-2011

Ali, R.S., Poll, C., Kandeler, E., 2018. Dynamics of soil respiration and microbial communities: Interactive controls of temperature and substrate quality. Soil Biol. Biochem. 127, 60–70. https://doi.org/10.1016/j.soilbio.2018.09.010

Alster, C.J., von Fischer, J.C., Allison, S.D., Treseder, K.K., 2020. Embracing a new paradigm for temperature sensitivity of soil microbes. Glob. Chang. Biol. 26, 3221–3229. https://doi.org/10.1111/gcb.15053

AminiTabrizi, R., Dontsova, K., Graf Grachet, N., Tfaily, M.M., 2022. Elevated temperatures drive abiotic and biotic degradation of organic matter in a peat bog under oxic conditions. Sci. Total Environ. 804, 150045. https://doi.org/10.1016/j.scitotenv.2021.150045

AminiTabrizi, R., Graf-Grachet, N., Chu, R.K., Toyoda, J.G., Hoyt, D.W., Hamdan, R., Wilson, R.M., Tfaily, M.M., 2023. Microbial sensitivity to temperature and sulfate deposition modulates greenhouse gas emissions from peat soils. Glob. Chang. Biol. 1–20. https://doi.org/10.1111/gcb.16614

Auffret, M.D., Karhu, K., Khachane, A., Dungait, J.A.J., Fraser, F., Hopkins, D.W., Wookey, P.A., Singh, B.K., Freitag, T.E., Hartley, I.P., Prosser, J.I., 2016. The role of microbial community composition in controlling soil respiration responses to temperature. PLoS One 11, 1–19. https://doi.org/10.1371/journal.pone.0165448

Baldrian, P., Kolaiřík, M., Štursová, M., Kopecký, J., Valášková, V., Větrovský, T., Žifčáková, L., Šnajdr, J., Rídl, J., Vlček, Č., Voříšková, J., 2012. Active and total microbial communities in forest soil are largely different and highly stratified during decomposition. ISME J. 6, 248–258. https://doi.org/10.1038/ismej.2011.95

Bao, K., Xia,W., Lu, X.,Wang, G., 2010a. Recent atmospheric lead deposition recorded in an ombrotrophic peat bog of Great Hinggan Mountains, Northeast China, from 210Pb and 137Cs dating. J. Environ. Radioact. 101, 773–779. https://doi.org/ 10.1016/j.jenvrad.2010.05.004

Beer J, Blodau C. Transport and thermodynamics constrain belowground carbon turnover in a northern peatland. Geochim. Cosmochim. Acta., 2007, 71(12): 2989-3002. https://doi.org/10.1016/j.gca.2007.03.010

Birnbaum, C., Wood, J., Lilleskov, E., Lamit, L.J., Shannon, J., Brewer, M., Grover, S., 2022. Degradation reduces microbial richness and alters microbial functions in an australian peatland. Microb. Ecol. https://doi.org/10.1007/s00248-022-02071-z

Bonaiuti, S., Blodau, C., Knorr, K.H., 2020. Evaluating biogeochemical indicators of methanogenic conditions and thermodynamic constraints in peat. Appl. Geochemistry 114, 104471. https://doi.org/10.1016/j.apgeochem.2019.104471

Bosatta, E., Ågren, G.I., 1999. Soil organic matter quality interpreted thermodynamically. Soil Biol. Biochem. 31, 1889–1891. https://doi.org/10.1016/S0038-0717(99)00105-4

Bragazza, L., Parisod, J., Buttler, A., Bardgett, R.D., 2013. Biogeochemical plant-soil microbe feedback in response to climate warming in peatlands. Nat. Clim. Chang. 3, 273–277. https://doi.org/10.1038/nclimate1781

Bridgham, S.D., Cadillo-Quiroz, H., Keller, J.K., Zhuang, Q., 2013. Methane emissions from wetlands:

Biogeochemical, microbial, and modeling perspectives from local to global scales. Glob. Chang. Biol. 19, 1325–1346. https://doi.org/10.1111/gcb.12131

Briones, M.J.I., Mcnamara, N.P., Poskitt, J., Crow, S.E., Ostle, N.J., 2014. Interactive biotic and abiotic regulators of soil carbon cycling: Evidence from controlled climate experiments on peatland and boreal soils. Glob. Chang. Biol. 20, 2971–2982. https://doi.org/10.1111/gcb.12585

Broder, T., Blodau, C., Biester, H., Knorr, K.H., 2012. Peat decomposition records in three pristine ombrotrophic bogs in southern Patagonia. Biogeosciences 9, 1479–1491. https://doi.org/10.5194/bg-9-1479-2012

Chen, J., Luo, Y., Sinsabaugh, R.L., 2023. Subsoil carbon loss 16, 284–285. https://doi.org/10.1038/s41561-023-01164-9

Chow, A.T., Tanji, K.K., Gao, S., Dahlgren, R.A., 2006. Temperature, water content and wet-dry cycle effects on DOC production and carbon mineralization in agricultural peat soils. Soil Biol. Biochem. 38, 477–488. https://doi.org/10.1016/j.soilbio.2005.06.005

Coates, J.D., Ellis, D.J., Gaw, C. V., Lovley, D.R., 1999. Geothrix fermentans gen. nov., sp. nov., a novel Fe(III)-reducing bacterium from a hydrocarbon-contaminated aquifer. Int. J. Syst. Bacteriol. 49, 1615–1622. https://doi.org/10.1099/00207713-49-4-1615

Cong, J., Gao, C., Ji, S., Li, X., Han, D., Wang, G., 2023. Changes in organic matter properties and carbon chemical stability in surface soils associated with changing vegetation communities in permafrost peatlands. Biogeochemistry. https://doi.org/10.1007/s10533-023-01028-9

Conrad, R., 2005. Quantification of methanogenic pathways using stable carbon isotopic signatures: A review and a proposal. Org. Geochem. 36, 739–752. https://doi.org/10.1016/j.orggeochem.2004.09.006

Conrad, R., 2020. Importance of hydrogenotrophic, aceticlastic and methylotrophic methanogenesis for methane production in terrestrial, aquatic and other anoxic environments: A mini review. Pedosphere 30, 25–39. https://doi.org/10.1016/S1002-0160(18)60052-9

Cory, R.M., McKnight, D.M., 2005. Fluorescence spectroscopy reveals ubiquitous presence of oxidized and reduced quinones in dissolved organic matter. Environ. Sci. Technol. 39, 8142–8149. https://doi.org/10.1021/es0506962

Coward, E.K., Thompson, A.T., Plante, A.F., 2017. Iron-mediated mineralogical control of organic matter accumulation in tropical soils. Geoderma 306, 206–216. https://doi.org/10.1016/j.geoderma.2017.07.026

Csardi, G., Nepusz, T., 2006. The igraph software package for complex network research. InterJournal, Complex Systems 1695, 1–9.

Davidson, E.A., Janssens, I.A., 2006. Temperature sensitivity of soil carbon decomposition and feedbacks to climate change. Nature 440, 165–173. https://doi.org/10.1038/nature04514

Davis, K.E.R., Sangwan, P., Janssen, P.H., 2011. Acidobacteria, Rubrobacteridae and Chloroflexi are abundant among very slow-growing and mini-colony-forming soil bacteria. Environ. Microbiol. 13, 798–805. https://doi.org/10.1111/j.1462-2920.2010.02384.x

Dedysh, S.N., 2011. Cultivating uncultured bacteria from northern wetlands: Knowledge gained and remaining gaps. Front. Microbiol. 2, 1–15. https://doi.org/10.3389/fmicb.2011.00184

Drake, T.W., Wickland, K.P., Spencer, R.G.M., McKnight, D.M., Striegl, R.G., 2015. Ancient low-molecular-weight organic acids in permafrost fuel rapid carbon dioxide production upon thaw. Proc. Natl. Acad. Sci. U. S. A. 112, 13946–13951. https://doi.org/10.1073/pnas.1511705112.

Fernandez, I., Mahieu, N. Cadisch, G. Carbon isotopic fractionation during decomposition of plant

materials of different quality. Glo. Biogeochem. Cyc. 17, 1075, doi: 10. 1029/2001GB001834 (2003).
Fierer, N., Bradford, M.A., Jackson, R.B., 2007. Toward an ecological classification of soil bacteria. Ecology 88, 1354–1364. https://doi.org/10.1890/05-1839
Fierer, N., Colman, B.P., Schimel, J.P., Jackson, R.B., 2006. Predicting the temperature dependence of microbial respiration in soil: A continental-scale analysis. Global Biogeochem. Cycles 20. https://doi.org/10.1029/2005GB002644
Frankenberg, C., Meirink, J.F., Van Weele, M., Platt, U., Wagner, T., 2005. Assessing methane emissions from global space-borne observations. Science. 308, 1010–1014. https://doi.org/10.1126/science.1106644
Gao, C., Knorr, K.H., Yu, Z., He, J., Zhang, S., Lu, X., Wang, G., 2016. Black carbon deposition and storage in peat soils of the Changbai Mountain, China. Geoderma 273, 98–105. https://doi.org/10.1016/j.geoderma.2016.03.021
Gao, C., Sander, M., Agethen, S., Knorr, K.H., 2019. Electron accepting capacity of dissolved and particulate organic matter control CO2 and CH4 formation in peat soils. Geochim. Cosmochim. Acta 245, 266–277. https://doi.org/10.1016/j.gca.2018.11.004
Gill, A.L., Giasson, M.A., Yu, R., Finzi, A.C., 2017. Deep peat warming increases surface methane and carbon dioxide emissions in a black spruce-dominated ombrotrophic bog. Glob. Chang. Biol. 23, 5398–5411. https://doi.org/10.1111/gcb.13806
Guth, P., Gao, C., Knorr, K. Electron accepting capacities of a wide variety of peat materials from around the globe similarly explain CO_2 and CH_4 Formation. https://doi.org/10.1029/2022GB007459
Harrell, F.E. Hmisc: Harrell Miscellaneous. R Package., 4.2-0. 2019. Available online: https://github.com/harrelfe/Hmisc/ (accessed on 3 December 2019).
Heslop, J.K., Winkel, M., Walter Anthony, K.M., Spencer, R.G.M., Podgorski, D.C., Zito, P., Kholodov, A., Zhang, M., Liebner, S., 2019. Increasing organic carbon biolability with depth in Yedoma permafrost: ramifications for future climate change. J. Geophys. Res. Biogeosciences 124, 2021–2038. https://doi.org/10.1029/2018JG004712
Hilasvuori, E., Akujärvi, A., Fritze, H., Karhu, K., Laiho, R., Mäkiranta, P., Oinonen, M., Palonen, V., Vanhala, P., Liski, J., 2013. Temperature sensitivity of decomposition in a peat profile. Soil Biol. Biochem. 67, 47–54. https://doi.org/10.1016/j.soilbio.2013.08.009
Hopple, A.M., Wilson, R.M., Kolton, M., Zalman, C.A., Chanton, J.P., Kostka, J., Hanson, P.J., Keller, J.K., Bridgham, S.D., 2020. Massive peatland carbon banks vulnerable to rising temperatures. Nat. Commun. 11, 4–10. https://doi.org/10.1038/s41467-020-16311-8
Hu, H., Wen, J., Peng, Z., Tian, F., Tie, Q., Lu, Y., Khan, M. Y. A. 2019. High-frequency monitoring of the occurrence of preferential flow on hillslopes and its relationship with rainfall features, soil moisture and landscape. Hydrological Sciences Journal. doi:10.1080/02626667.2019.1638.
Jackson, C.R., Tyler, H.L., Millar, J.J., 2013. Determination of microbial extracellular enzyme activity in waters, soils, and sediments using high throughput microplate assays. J. Vis. Exp. 1–9. https://doi.org/10.3791/50399.
Khan, M. Y. A., Tian, F., 2018. Understanding the potential sources and environmental impacts of dissolved and suspended organic carbon in the diversified Ramganga River, Ganges Basin, India, Proc. IAHS, 379, 61–66. https://doi.org/10.5194/piahs-379-61-2018.
Kluber, L.A., Johnston, E.R., Allen, S.A., Nicholas Hendershot, J., Hanson, P.J., Schadt, C.W., 2020.

Constraints on microbial communities, decomposition and methane production in deep peat deposits. PLoS One 15, 1–20. https://doi.org/10.1371/journal.pone.0223744.

Kumar, A., Mishra, S., Pandey, R., Yu, Zhiguo., et al., 2022. Microplastics in terrestrial ecosystems: Un-ignorable impacts on soil characterises, nutrient storage and its cycling. TrAC Trends in Analytical Chemistry, 158, 116869. https://doi.org/10.1016/j.trac.2022.116869.

Lamit, L.J., Romanowicz, K.J., Potvin, L.R., Lennon, J.T., Tringe, S.G., Chimner, R.A., Kolka, R.K., Kane, E.S., Lilleskov, E.A., 2021. Peatland microbial community responses to plant functional group and drought are depth-dependent. Mol. Ecol. 30, 5119–5136. https://doi.org/10.1111/mec.16125

Leifeld, J., Menichetti, L., 2018. The underappreciated potential of peatlands in global climate change mitigation strategies /704/47/4113 /704/106/47 article. Nat. Commun. 9. https://doi.org/10.1038/s41467-018-03406-6

Li, H., Yang, S., Semenov, M. V., Yao, F., Ye, J., Bu, R., Ma, R., Lin, J., Kurganova, I., Wang, X., Deng, Y., Kravchenko, I., Jiang, Y., Kuzyakov, Y., 2021. Temperature sensitivity of SOM decomposition is linked with a K-selected microbial community. Glob. Chang. Biol. 27, 2763–2779. https://doi.org/10.1111/gcb.15593

Li, Q., Leroy, F., Zocatelli, R., Gogo, S., Jacotot, A., Guimbaud, C., Laggoun-Défarge, F., 2021. Abiotic and biotic drivers of microbial respiration in peat and its sensitivity to temperature change. Soil Biol. Biochem. 153, 108077. https://doi.org/10.1016/j.soilbio.2020.108077

Li, X.M., Chen, Q.L., He, C., Shi, Q., Chen, S.C., Reid, B.J., Zhu, Y.G., Sun, G.X., 2019. Organic Carbon Amendments Affect the Chemodiversity of Soil Dissolved Organic Matter and Its Associations with Soil Microbial Communities. Environ. Sci. Technol. 53, 50–59. https://doi.org/10.1021/acs.est.8b04673

Limpens, J., Berendse, F., Blodau, C., Canadell, J.G., Freeman, C., Holden, J., Roulet, N., Rydin, H., Schaepman-Strub, G., 2008. Peatlands and the carbon cycle: From local processes to global implications - A synthesis. Biogeosciences 5, 1475–1491. https://doi.org/10.5194/bg-5-1475-2008

Lin, X., Green, S., Tfaily, M.M., Prakash, O., Konstantinidis, K.T., Corbett, J.E., Chanton, J.P., Cooper, W.T., Kostka, J.E., 2012. Microbial community structure and activity linked to contrasting biogeochemical gradients in bog and fen environments of the glacial lake agassiz peatland. Appl. Environ. Microbiol. 78, 7023–7031. https://doi.org/10.1128/AEM.01750-12

Lin, X., Tfaily, M.M., Steinweg, J.M., Chanton, P., Esson, K., Yang, Z.K., Chanton, J.P., Cooper, W., Schadt, C.W., Kostka, J.E., 2014. Microbial community stratification linked to utilization of carbohydrates and phosphorus limitation in a Boreal Peatland at Marcell Experimental Forest, Minnesota, USA. Appl. Environ. Microbiol. 80, 3518–3530. https://doi.org/10.1128/AEM.00205-14

Lipson, D.A., Haggerty, J.M., Srinivas, A., Raab, T.K., Sathe, S., Dinsdale, E.A., 2013. Metagenomic Insights into anaerobic metabolism along an arctic peat soil profile. PLoS One 8. https://doi.org/10.1371/journal.pone.0064659

Liu, L., Chen, H., Zhu, Q., Yang, G., Zhu, E., Hu, J., Peng, C., Jiang, L., Zhan, W., Ma, T., He, Y., Zhu, D., 2016. Responses of peat carbon at different depths to simulated warming and oxidizing. Sci. Total Environ. 548–549, 429–440. https://doi.org/10.1016/j.scitotenv.2015.11.149

Logue, J.B., Stedmon, C. a, Kellerman, A.M., Nielsen, N.J., Andersson, A.F., Laudon, H., Lindström, E.S., Kritzberg, E.S., 2015. Experimental insights into the importance of aquatic bacterial

community composition to the degradation of dissolved organic matter. ISME J. 1–13. https://doi.org/10.1038/ismej.2015.131

Loisel, J., Yu, Z., Beilman, D.W., Camill, P., Alm, J., Amesbury, M.J., Anderson, D., Andersson, S., Bochicchio, C., Barber, K., Belyea, L.R., Bunbury, J., Chambers, F.M., Charman, D.J., De Vleeschouwer, F., Fiałkiewicz-Kozieł, B., Finkelstein, S.A., Gałka, M., Garneau, M., Hammarlund, D., Hinchcliffe, W., Holmquist, J., Hughes, P., Jones, M.C., Klein, E.S., Kokfelt, U., Korhola, A., Kuhry, P., Lamarre, A., Lamentowicz, M., Large, D., Lavoie, M., MacDonald, G., Magnan, G., Mäkilä, M., Mallon, G., Mathijssen, P., Mauquoy, D., McCarroll, J., Moore, T.R., Nichols, J., O'Reilly, B., Oksanen, P., Packalen, M., Peteet, D., Richard, P.J.H., Robinson, S., Ronkainen, T., Rundgren, M., Sannel, A.B.K., Tarnocai, C., Thom, T., Tuittila, E.S., Turetsky, M., Väliranta, M., van der Linden, M., van Geel, B., van Bellen, S., Vitt, D., Zhao, Y., Zhou, W., 2014. A database and synthesis of northern peatland soil properties and Holocene carbon and nitrogen accumulation. Holocene 24, 1028–1042. https://doi.org/10.1177/0959683614538073

Lü, W., Ren, H., Ding, W., Li, H., Yao, X., Jiang, X., Qadeer, A., 2022. Biotic and abiotic controls on sediment carbon dioxide and methane fluxes under short-term experimental warming. Water Res. 226, 119312. https://doi.org/10.1016/j.watres.2022.119312

Mao, X., Zheng, J., Yu, W., Guo, X., Xu, K., Zhao, R., Xiao, L., Wang, M., Jiang, Y., Zhang, S., Luo, L., Chang, J., Shi, Z., Luo, Z., 2022. Climate-induced shifts in composition and protection regulate temperature sensitivity of carbon decomposition through soil profile. Soil Biol. Biochem. 172. https://doi.org/10.1016/j.soilbio.2022.108743

Mehta-Kolte, M.G., Bond, D.R., 2012. Geothrix fermentans secretes two different redox-active compounds to utilize electron acceptors across a wide range of redox potentials. Appl. Environ. Microbiol. 78, 6987–6995. https://doi.org/10.1128/AEM.01460-12

Ming, G., Hu, H., Tian, F., Khan, M. Y. A., Zhang, Q. (2021). Carbon budget for a plastic-film mulched and drip-irrigated cotton field in an oasis of Northwest China. Agric For Meteorol., 306, 108447.

Niemeyer, J., Chen, Y., Bollag, J.-M., 1992. Characterization of humic acids, composts, and peat by diffuse reflectance fourier-transform infrared spectroscopy. Soil Sci. Soc. Am. J. 56, 135–140. https://doi.org/10.2136/sssaj1992.03615995005600010021x

Pankratov, T.A., Serkebaeva, Y.M., Kulichevskaya, I.S., Liesack, W., Dedysh, S.N., 2008. Substrate-induced growth and isolation of Acidobacteria from acidic Sphagnum peat. ISME J. 2, 551–560. https://doi.org/10.1038/ismej.2008.7

Schmidt, O., Horn, M.A., Kolb, S., Drake, H.L., 2015. Temperature impacts differentially on the methanogenic food web of cellulose-supplemented peatland soil. Environ. Microbiol. 17, 720–734. https://doi.org/10.1111/1462-2920.12507

Sihi, D., Inglett, P.W., Gerber, S., Inglett, K.S., 2018. Rate of warming affects temperature sensitivity of anaerobic peat decomposition and greenhouse gas production. Glob. Chang. Biol. 24, e259–e274. https://doi.org/10.1111/gcb.13839

Sihi, D., Inglett, P.W., Inglett, K.S., 2016. Carbon quality and nutrient status drive the temperature sensitivity of organic matter decomposition in subtropical peat soils. Biogeochemistry 131, 103–119. https://doi.org/10.1007/s10533-016-0267-8

Song, Y., Song, C., Hou, A., Ren, J., Wang, X., Cui, Q., Wang, M., 2018. Effects of temperature and root additions on soil carbon and nitrogen mineralization in a predominantly permafrost peatland.

776 Catena 165, 381–389. https://doi.org/10.1016/j.catena.2018.02.026
777 Stedmon, C.A., Markager, S., 2005. Resolving the variability in dissolved organic matter fluorescence
778 in a temperate estuary and its catchment using PARAFAC analysis. Limnol. Oceanogr. 50, 686–
779 697. https://doi.org/10.4319/lo.2005.50.2.0686
780 Stedmon, C.A., Markager, S., Bro, R., 2003. Tracing dissolved organic matter in aquatic environments
781 using a new approach to fluorescence spectroscopy. Mar. Chem. 82, 239–254.
782 https://doi.org/10.1016/S0304-4203(03)00072-0
783 Steinweg, J.M., Kostka, J.E., Hanson, P.J., Schadt, C.W., 2018a. Temperature sensitivity of
784 extracellular enzymes differs with peat depth but not with season in an ombrotrophic bog. Soil
785 Biol. Biochem. 125, 244–250. https://doi.org/10.1016/j.soilbio.2018.07.001
786 Steinweg, J.M., Kostka, J.E., Hanson, P.J., Schadt, C.W., 2018b. Temperature sensitivity of
787 extracellular enzymes differs with peat depth but not with season in an ombrotrophic bog. Soil
788 Biol. Biochem. 125, 244–250. https://doi.org/10.1016/j.soilbio.2018.07.001
789 Tfaily, M.M., Cooper, W.T., Kostka, J.E., Chanton, P.R., Schadt, C.W., Hanson, P.J., Iversen, C.M.,
790 Chanton, J.P., 2014. Organic matter transformation in the peat column at Marcell Experimental
791 Forest: Humification and vertical stratification. J. Geophys. Res. Biogeosciences 119, 661–675.
792 https://doi.org/10.1002/2013JG002492
793 Tfaily, M.M., Corbett, J.E., Wilson, R., Chanton, J.P., Glaser, P.H., Cawley, K.M., Jaffé, R., Cooper,
794 W.T., 2015. Utilization of PARAFAC-modeled excitation-emission matrix (EEM) fluorescence
795 spectroscopy to identify biogeochemical processing of dissolved organic matter in a Northern
796 peatland. Photochem. Photobiol. 91, 684–695. https://doi.org/10.1111/php.12448
797 Thauer, R.K., Kaster, A.K., Seedorf, H., Buckel, W., Hedderich, R., 2008. Methanogenic archaea:
798 Ecologically relevant differences in energy conservation. Nat. Rev. Microbiol. 6, 579–591.
799 https://doi.org/10.1038/nrmicro1931
800 Tong, D., Li, Z., Xiao, H., Nie, X., Liu, C., Zhou, M., 2021. How do soil microbes exert impact on soil
801 respiration and its temperature sensitivity? Environ. Microbiol. 23, 3048–3058.
802 https://doi.org/10.1111/1462-2920.15520
803 Urbanová, Z., Bárta, J., 2014. Microbial community composition and in silico predicted metabolic
804 potential reflect biogeochemical gradients between distinct peatland types. FEMS Microbiol.
805 Ecol. 90, 633–646. https://doi.org/10.1111/1574-6941.12422
806 Verbeke, B.A., Lamit, L.J., Lilleskov, E.A., Hodgkins, S.B., Basiliko, N., Kane, E.S., Andersen, R.,
807 Artz, R.R.E., Benavides, J.C., Benscoter, B.W., Borken, W., Bragazza, L., Brandt, S.M., Bräuer,
808 S.L., Carson, M.A., Charman, D., Chen, X., Clarkson, B.R., Cobb, A.R., Convey, P., Pasquel, J.
809 del Á., Enriquez, A.S., Griffiths, H., Grover, S.P., Harvey, C.F., Harris, L.I., Hazard, C.,
810 Hodgson, D., Hoyt, A.M., Hribljan, J., Jauhiainen, J., Juutinen, S., Knorr, K.H., Kolka, R.K.,
811 Könönen, M., Larmola, T., McCalley, C.K., McLaughlin, J., Moore, T.R., Mykytczuk, N.,
812 Normand, A.E., Rich, V., Roulet, N., Royles, J., Rutherford, J., Smith, D.S., Svenning, M.M.,
813 Tedersoo, L., Thu, P.Q., Trettin, C.C., Tuittila, E.S., Urbanová, Z., Varner, R.K., Wang, M.,
814 Wang, Z., Warren, M., Wiedermann, M.M., Williams, S., Yavitt, J.B., Yu, Z.G., Yu, Z.,
815 Chanton, J.P., 2022. Latitude, elevation, and mean annual temperature predict peat organic matter
816 chemistry at a global scale. Global Biogeochem. Cycles 36, 1–17.
817 https://doi.org/10.1029/2021GB007057
818 Viollier, E., Inglett, P.W., Hunter, K., Roychoudhury, A.N., Van Cappellen, P., 2000. The Ferrozine
819 method revisited: Fe (II)/Fe (III) determination in natural waters. Appl. Geochemistry 15, 785–

790. https://doi.org/10.1016/S0883-2927(99)00097-9
Wang, H.Y., Byrne, J.M., Perez, J.P.H., Thomas, A.N., Goettlicher, J., Hofer, H.E., Mayanna, S., Kontny, A., Kappler, A., Guo, H.M., Benning, L.G., Norra, S., 2020. Arsenic sequestration in pyrite and greigite in the buried peat of As-contaminated aquifers. Geochim. Cosmochim. Acta 284, 107–119. https://doi.org/10.1016/j.gca.2020.06.021
Wang, W., Tao, J., Yu, K., He, C., Wang, J., Li, P., Chen, H., Xu, B., Shi, Q., Zhang, C., 2021. Vertical stratification of dissolved organic matter linked to distinct microbial communities in subtropic estuarine sediments. Front. Microbiol. 12, 1–14. https://doi.org/10.3389/fmicb.2021.697860
Weishaar, J.L., Aiken, G.R., Bergamaschi, B.A., Fram, M.S., Fujii, R., Mopper, K., 2003. Evaluation of specific ultraviolet absorbance as an indicator of the chemical composition and reactivity of dissolved organic carbon. Environ. Sci. Technol. 37, 4702–4708. https://doi.org/10.1021/es030360x
Whiticar, M.J., 1999. Carbon and hydrogen isotope systematics of bacterial formation and oxidation of methane. Chem. Geol. 161, 291–314. https://doi.org/10.1016/S0009-2541(99)00092-3
Wilson, R.M., Hopple, A.M., Tfaily, M.M., Sebestyen, S.D., Schadt, C.W., Pfeifer-Meister, L., Medvedeff, C., Mcfarlane, K.J., Kostka, J.E., Kolton, M., Kolka, R.K., Kluber, L.A., Keller, J.K., Guilderson, T.P., Griffiths, N.A., Chanton, J.P., Bridgham, S.D., Hanson, P.J., 2016. Stability of peatland carbon to rising temperatures. Nat. Commun. 7, 1–10. https://doi.org/10.1038/ncomms13723
Yang, S., Liebner, S., Svenning, M.M., Tveit, A.T., 2021. Decoupling of microbial community dynamics and functions in Arctic peat soil exposed to short term warming. Mol. Ecol. 30, 5094–5104. https://doi.org/10.1111/mec.16118
Yu, Z., Loisel, J., Brosseau, D.P., Beilman, D.W., Hunt, S.J., 2010. Global peatland dynamics since the Last Glacial Maximum. Geophys. Res. Lett. 37, 1–5. https://doi.org/10.1029/2010GL043584
Zhang, L., Gałka, M., Kumar, A., Liu, M., Knorr, K.H., Yu, Z.G., 2021. Plant succession and geochemical indices in immature peatlands in the Changbai Mountains, northeastern region of China: Implications for climate change and peatland development. Sci. Total Environ. 773. https://doi.org/10.1016/j.scitotenv.2020.143776
Zhou, J., Deng, Y., Shen, L., Wen, C., Yan, Q., Ning, D., Qin, Y., Xue, K., Wu, L., He, Z., Voordeckers, J.W., Van Nostrand, J.D., Buzzard, V., Michaletz, S.T., Enquist, B.J., Weiser, M.D., Kaspari, M., Waide, R., Yang, Y., Brown, J.H., 2016. Temperature mediates continental-scale diversity of microbes in forest soils. Nat. Commun. 7. https://doi.org/10.1038/ncomms12083
Zosso, C.U., Ofiti, N.O.E., Torn, M.S., Wiesenberg, G.L.B., Schmidt, M.W.I., 2023. Rapid loss of complex polymers and pyrogenic carbon in subsoils under whole-soil warming. Nat. Geosci. 16. https://doi.org/10.1038/s41561-023-01142-1

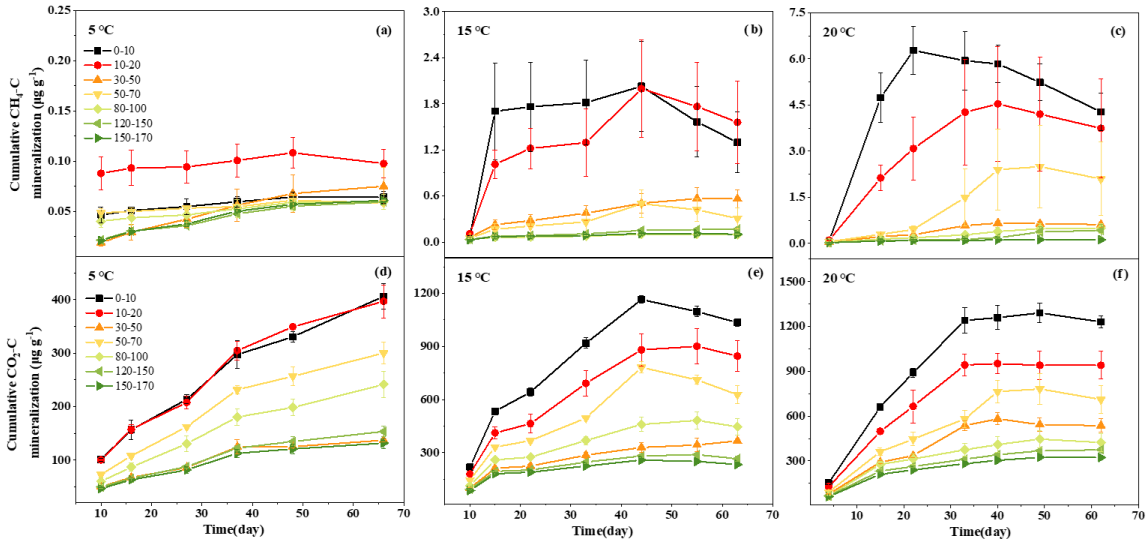

861

862 **Fig. 1** Cumulative CH_4 and CO_2 mineralization content in the vertical peat profiles

863 under different temperatures

864

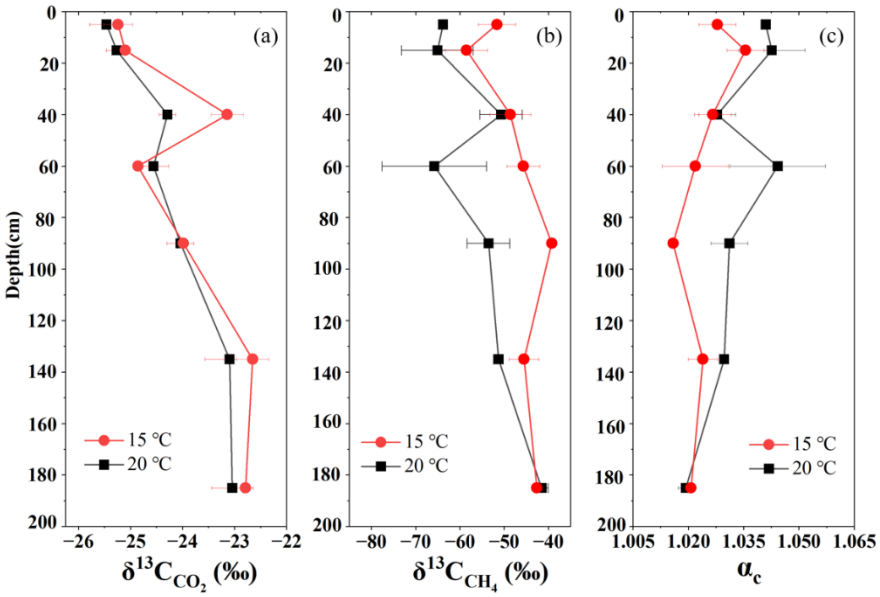

865

866 **Fig. 2** The $\delta^{13}C$ isotope signature in CO_2 and CH_4 and fractionation factor (α_c) of

867 vertical peat profiles at 15°C and 20°C

868

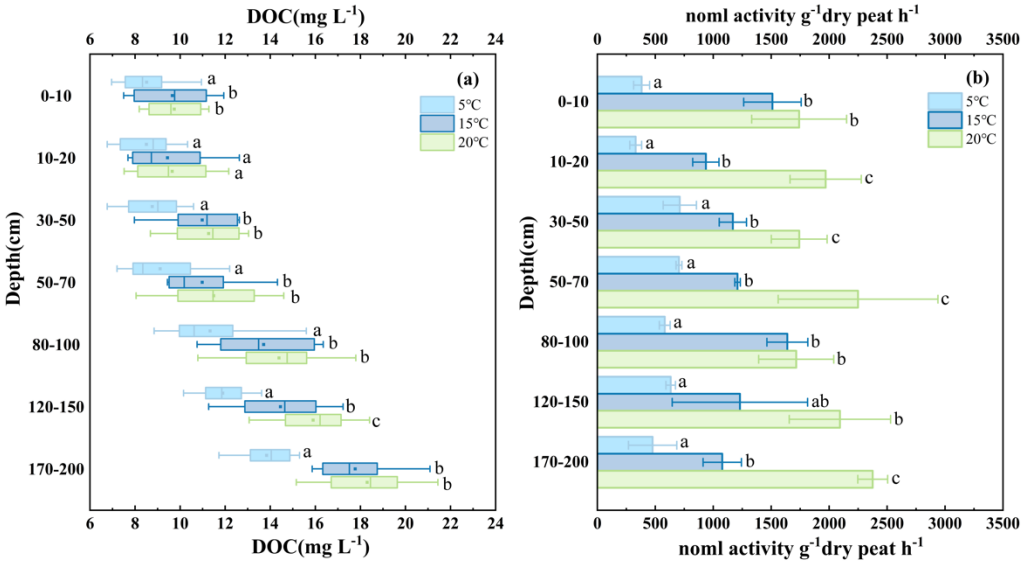

869

870 **Fig. 3** Variations of DOC concentration (a) and BG enzymatic activities (b) during the

871 entire incubation stage in vertical depth profiles under different temperatures

872

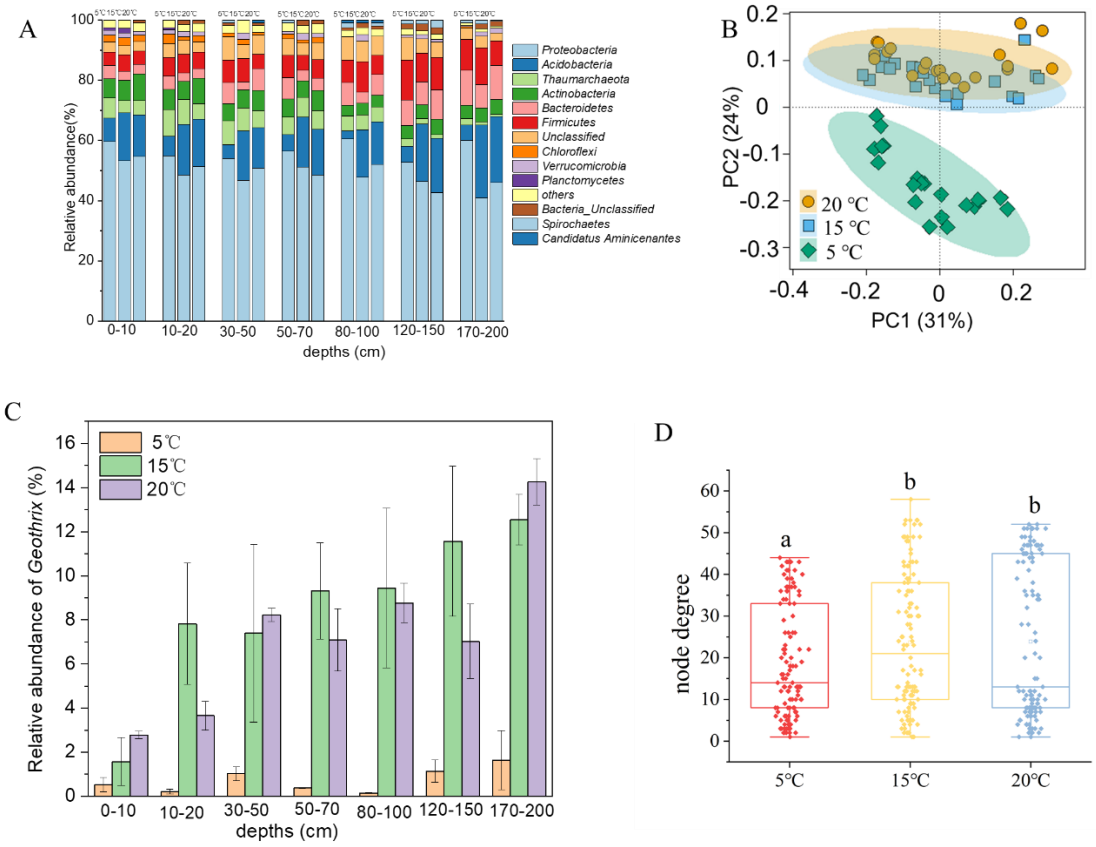

873

874

875 **Fig. 4** Microbial structure of peat samples in vertical profiles at 5°C, 15°C and 15°C.

876 (A) Top 10 phylum, (B) Principal coordinate analysis (PCoA) representing beta

877 diversity based on Bray-Curtis dissimilarity of bacterial communities, the bacterial

878 communities were grouped according to different temperature, (C) Relative abundance

879 of genus *Geothrix*, (D) node degree distributions under different temperature

880

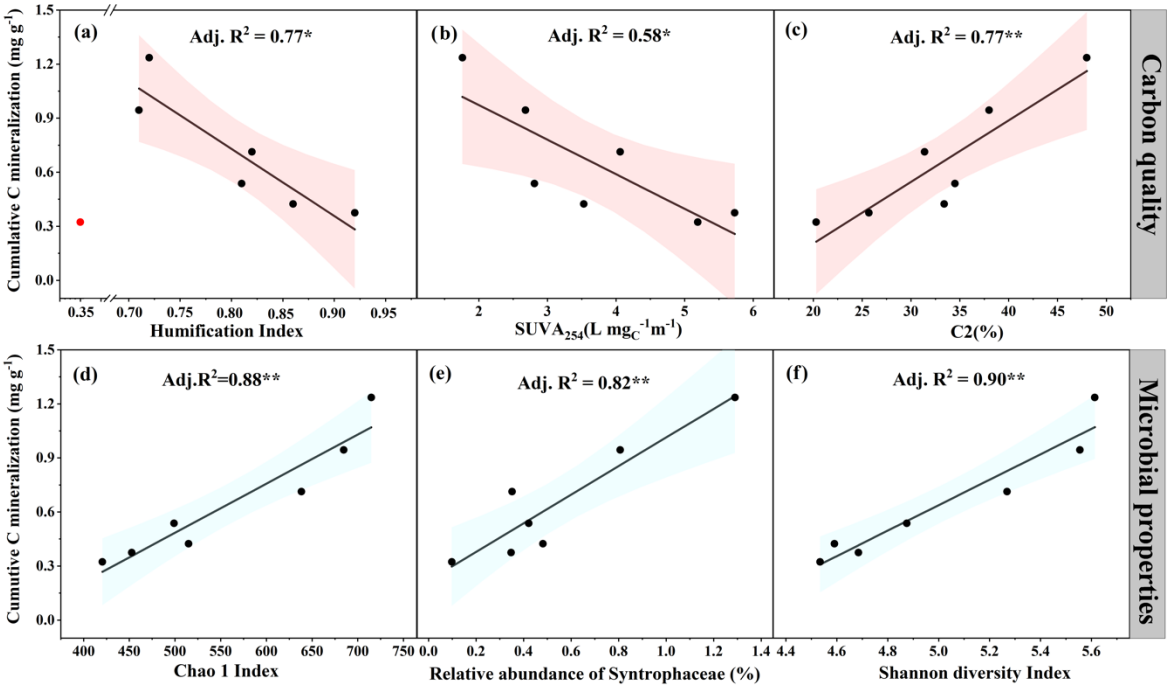

881

882

883 **Fig. 5** Correlations between cumulative carbon mineralization content and carbon

884 quality (a, b, c) as well as microbial properties (d, e, f). Point marked with red color in

885 Fig.a denote deviations.

886

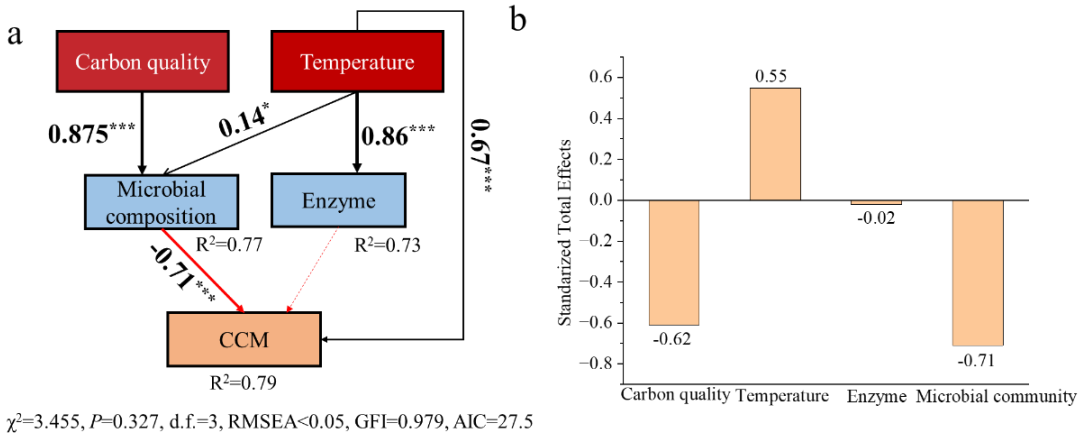

887
888

889 **Fig. 6** Structural equation models (SEM) revealing interactions of carbon quality and
890 microbial communities controlling CCM (CCM) and temperature effect (a) and
891 standardized total effects of each factor on CCM from SEM (b) $SUVA_{245}$ (Specific UV
892 absorbance at 254 nm) was used to standard for carbon quality. The solid black and red
893 arrows represent positive and negative correlations, while the dashed red lines indicate
894 non-significant correlations. The widths of arrows indicate the approximate strength. *
895 $p < 0.05$; ** $p < 0.01$; *** $p < 0.001$. A total 63 samples were included in the SEM
896 analysis.
897

898

899 **Table 1** Geochemical properties of peat samples in vertical profiles

Depth (cm)	C (%)	N (%)	C:N ratio	HI	Fe_{DCB} (g kg^{-1})[a]	OC_{DCB} (g kg^{-1})[b]	WEOC (mg L^{-1})[c]	$SUVA_{254}$ index ($mg_C^{-1}m^{-1}$)[d]	EEM C2 (%)[e]
0-10	34.56	2.20	15.71	0.72	1.67	11.4	13.32	1.76	48.0
10-20	43.29	2.18	19.86	0.71	1.01	8.43	6.71	2.68	38.0
30-50	43.17	2.07	20.86	0.81	0.68	7.90	6.24	2.81	34.5
50-70	41.17	2.10	19.60	0.82	0.86	8.90	6.47	4.06	31.4
80-100	44.03	2.33	18.90	0.86	0.66	9.73	7.44	3.53	33.4
120-150	44.94	2.14	21.00	0.92	0.44	9.53	9.44	5.73	25.7
170-200	45.00	2.18	20.64	0.35	0.52	8.39	7.32	5.19	20.3

900 a: Dithionite-citrate-bicarbonate (DCB) extractable Fe content in dry peat, b: DCB-extractable organic carbon
901 content in dry peat, c: water extractable organic carbon (WEOC) content in dry peat d, e: aromaticity ($SUVA_{254}$) and
902 ratio of protein-like components (C2) in WEOC
903
904
905
906

907 **Table 2** Summary of cumulative carbon mineralization, and temperature sensitivities
908 (Q_{10}) in vertical peat profiles
909

Depth (cm)	Cumulative carbon mineralization (CCM)							
	5°C		15°C		20°C			
	Total C (mg g^{-1})	P_{CH4} (%)	Total C (mg g^{-1})	P_{CH4} (%)	Total C (mg g^{-1})	P_{CH4} (%)	$Q_{1015\text{-}5°C}$	$Q_{1020\text{-}15°C}$
0-10	0.41 ± 0.024	0.02	1.04 ± 0.022	0.13	1.24 ± 0.037	0.35	2.56 ± 0.14a	1.42 ± 0.03a
10-20	0.40 ± 0.031	0.02	0.85 ± 0.087	0.18	0.94 ± 0.094	0.40	2.13 ± 0.12b	1.30 ± 0.45a
30-50	0.14 ± 0.003	0.05	0.37 ± 0.009	0.15	0.54 ± 0.045	0.11	2.68 ± 0.05a	2.14 ± 0.25b
50-70	0.30 ± 0.02	0.02	0.63 ± 0.051	0.05	0.71 ± 0.09	0.29	2.09 ± 0.11b	1.29 ± 0.15a
80-100	0.24 ± 0.024	0.02	0.45 ± 0.047	0.02	0.42 ± 0.06	0.11	1.87 ± 0.34c	0.96 ± 0.41a
120-150	0.15 ± 0.01	0.04	0.27 ± 0.013	0.06	0.37 ± 0.015	0.11	1.73 ± 0.03c	2.01 ± 0.33b
170-200	0.13 ± 0.01	0.05	0.23 ± 0.005	0.04	0.32 ± 0.002	0.04	1.77 ±0.14c	1.92 ± 0.07b

910
911
912
913

Supplementary materials

915

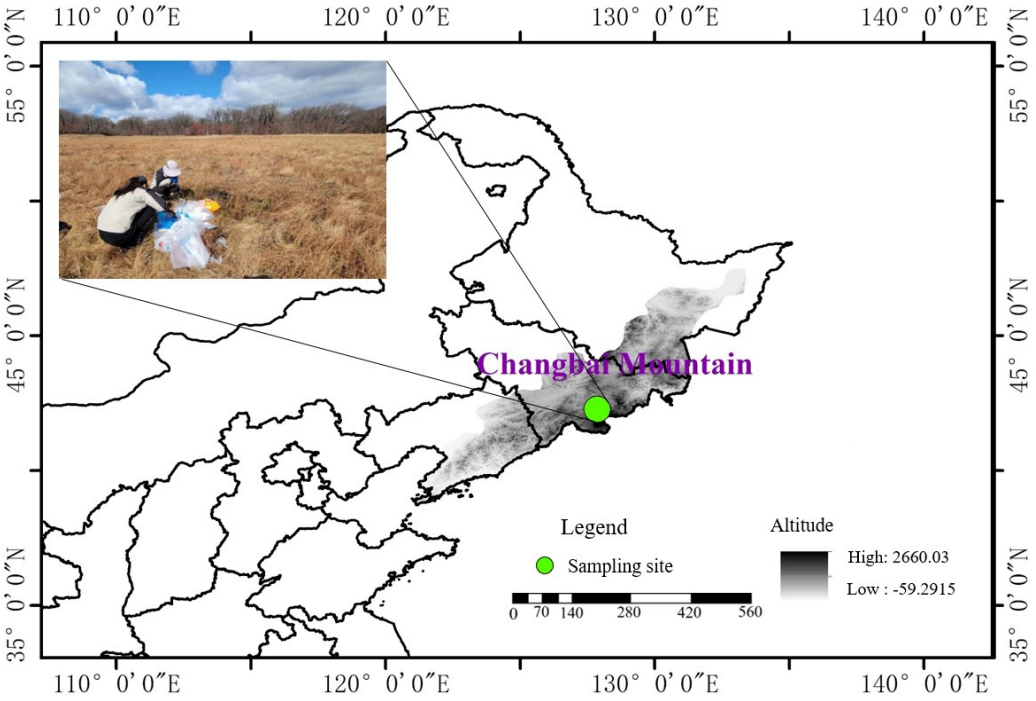

916

917 **Fig. S1** Location of the study area

918

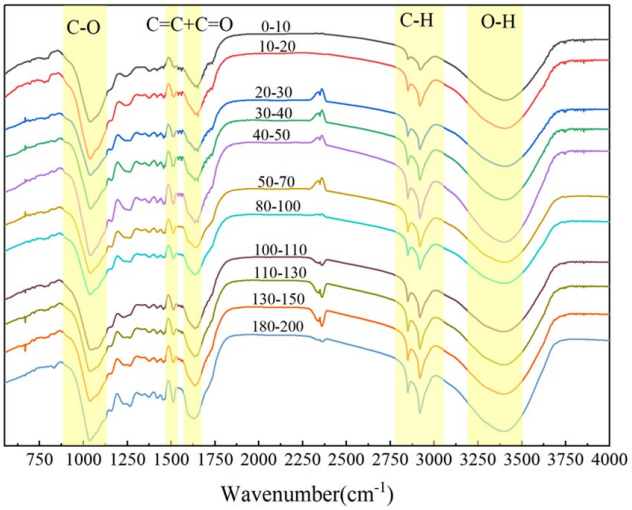

Fig. S2 FTIR spectra of peat samples in vertical peat profiles

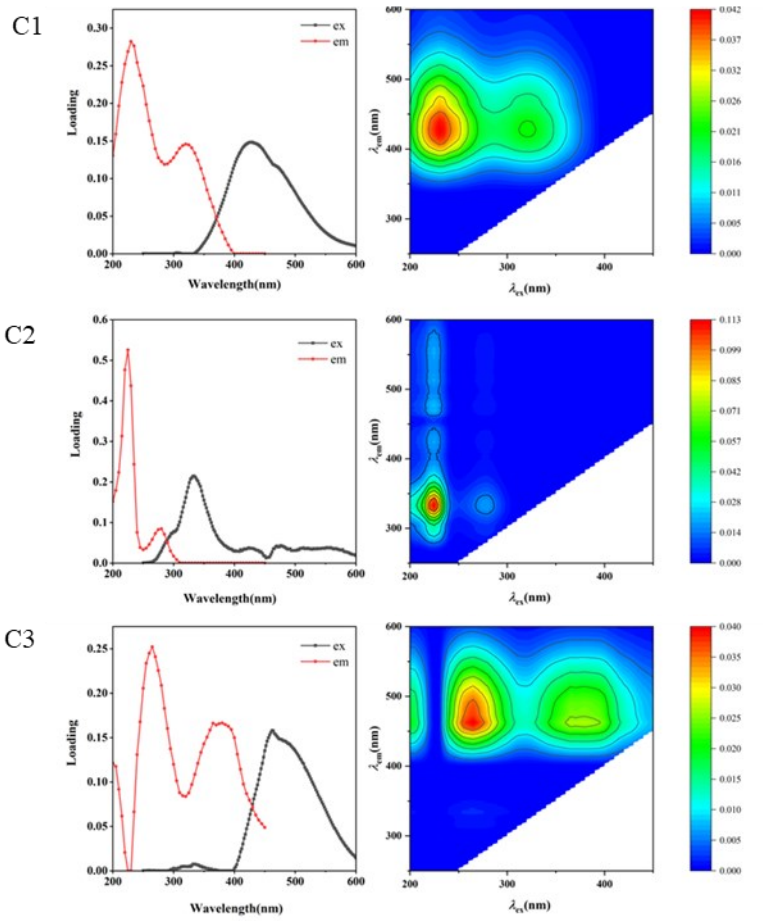

Fig. S3 Dissolved organic carbon (DOC) properties of three fluorophores identified by parallel factor analysis (PARAFAC)

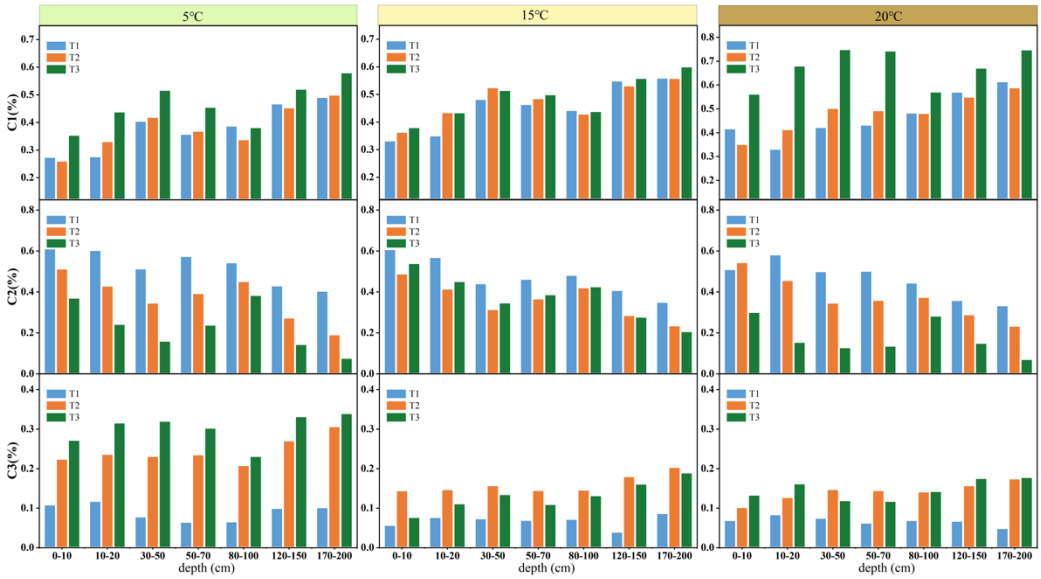

Fig. S4 Variations of organic carbon properties identified by excitation-emission matrix fluorescence spectroscopy coupled to parallel factor analysis (EEMs-PARAFAC) (T1: 10 day, T2: 25 day, T3: 70 day)

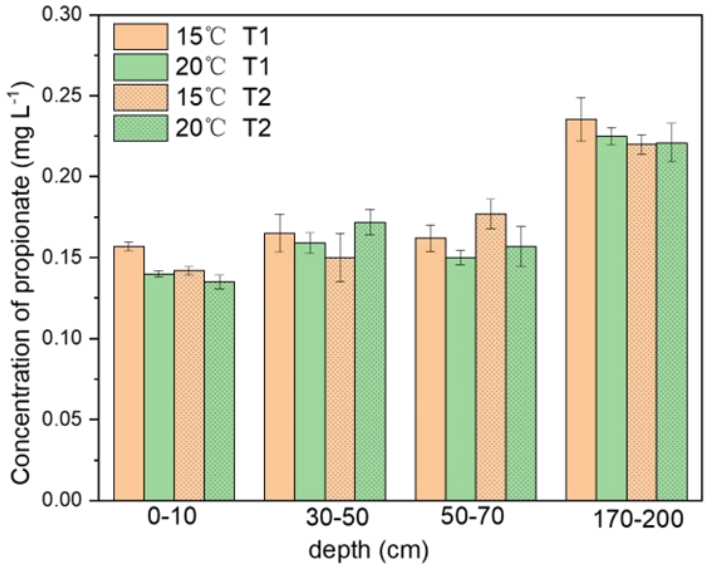

933

934

935 **Fig. S5** Concentration of propionate in the selective samples of 15°C and 20°C under specific time

936 (T1:10 day, T2:25 day)

937

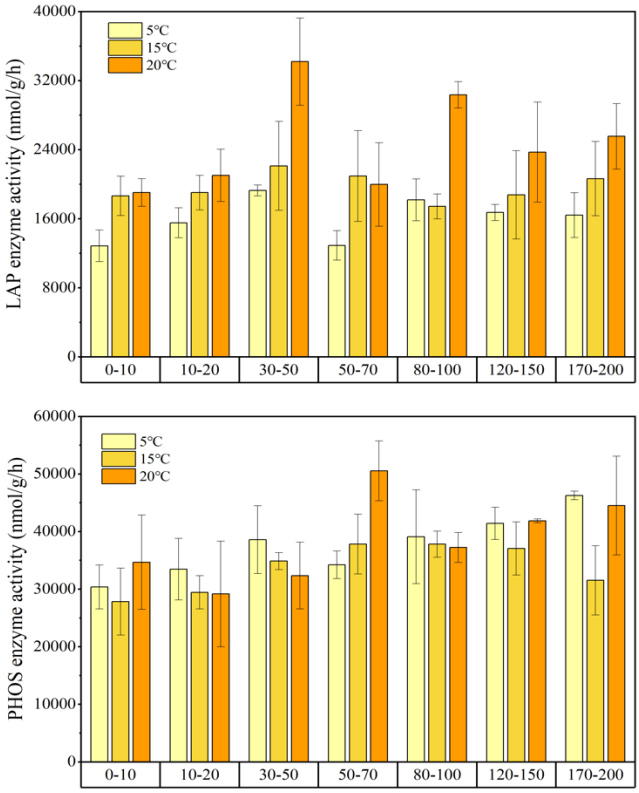

Fig. S6 Leucine-amino peptidase **(**LAP) and acid phosphor-monoesterase (PHOS) enzymatic activities in peat samples of vertical profile at different temperatures. LAP: leucine-amino peptidase. PHOS: acid phospho-monoesterase.

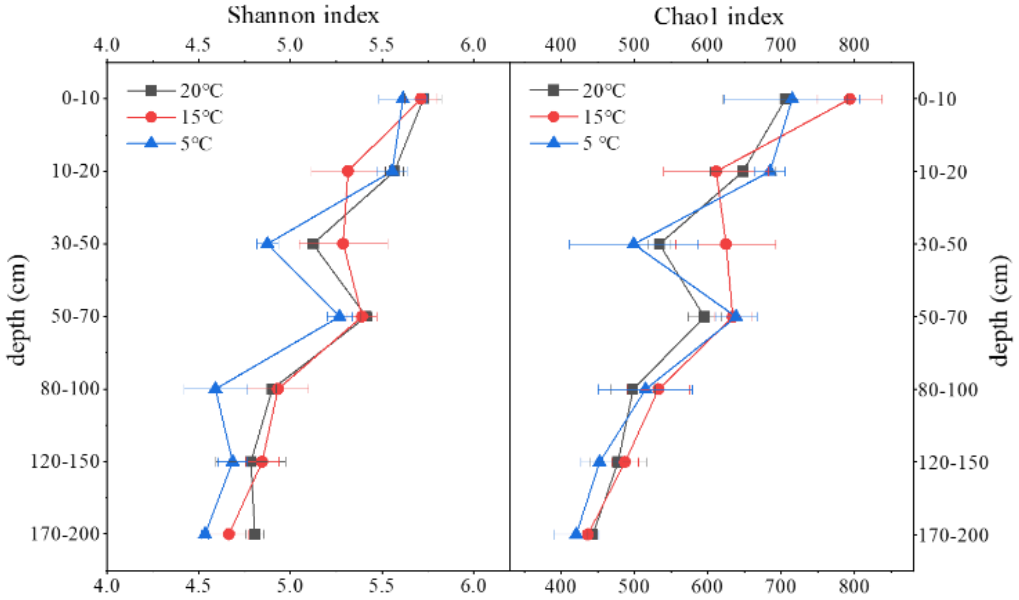

943

944 **Fig. S7** The Shannon and Chao 1 index of microbial communities in each peat sample of different
945 temperatures.

946

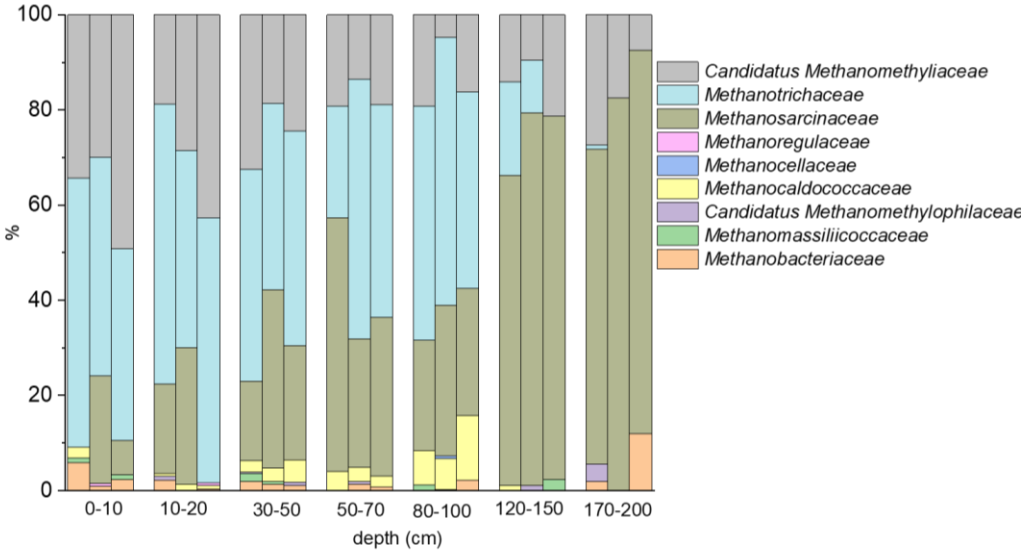

947

948 **Fig. S8** Relative abundances of methanogens in depth profiles under different temperatures

949

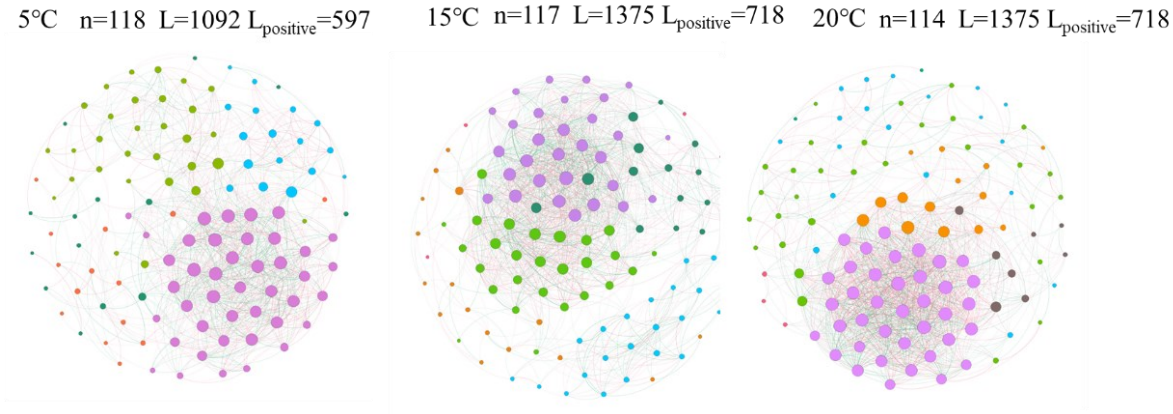

Fig. S9 Network analysis of microbial communities at genus level for peat samples under different incubation temperatures

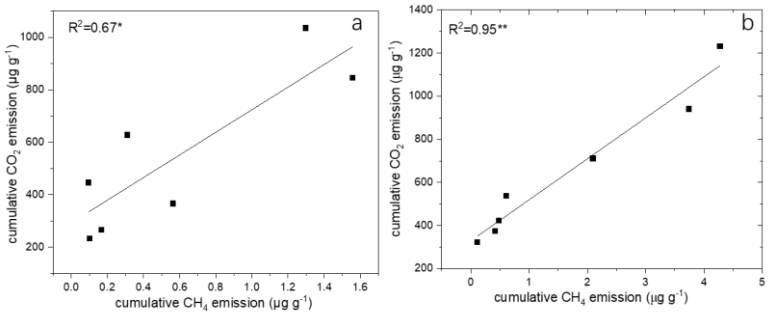

Fig. S10 Correlations between cumulative CH_4 emission and CO_2 emission at 15°C (a) and 20°C (b)

959

960 **Table S1** PCR thermal programs for 16S rRNA sequencing

Target gene	**Reaction mixture**	**Volumes[μl]**	**Thermal program**	
16S rRNA genes of becteria	5×FastPfu Buffer	4 μl	Cycles at:	95°C - 5 min
	515F	0.8μl (5 μM)		95°C - 30 s
	806R	0.8μl (5 μM)		58°C - 30 s
	FastPfu Polymerase	0.4 μl		72°C - 45 s
	dNTPs	2 μl (2.5 mM)		72°C - 10 min
	Template	1 (10 ng)		
	PCR water	11		

961

962

963

964

965 **Table S2** The DOC components identified by PARAFAC analysis

966

Component	Excitation maxima(nm)	Emission maxima(nm)	Possible source/classes of compound
C1	230/330	430	Terrestrial humic-like component (D'Andrilli et al., 2019) (Zhuang et al., 2021), with high molecular weight degraded from lignin (Zhou et al., 2019)
C2	225/275	332	Protein-tryptophan-like component (Gao and Guéguen, 2017), tryptophan-like component was linked to biological production (Cole et al., 2006), fresh autochthonous DOM (Zhou et al., 2019)
C3	270/380	480	Terrestrial reduced quinine-like compounds (Cory and McKnight, 2005; Tfaily et al., 2015)

967

968

Table S3 Cumulative carbon decomposition content (sum of DOC, CH_4 and CO_2) of peat samples in vertical profile

Depth (cm)	5°C (mg g^{-1})	15°C (mg g^{-1})	20°C (mg g^{-1})
0-10	1.5 ± 0.08	2.3 ± 0.06	2.5 ± 0.04
10-20	1.4 ± 0.07	2.0 ± 0.1	2.1 ± 0.1
30-50	1.1 ± 0.02	1.6 ± 0.02	1.8 ± 0.04
50-70	1.4 ± 0.03	2.0 ± 0.15	2.1 ± 0.09
80-100	1.4 ± 0.13	1.8 ± 0.05	1.8 ± 0.07
120-150	1.4 ± 0.06	1.7 ± 0.03	2.0 ± 0.04
170-200	1.3 ± 0.03	1.7 ± 0.04	1.8 ± 0.04

Table S4 Summary of Q_{10} of anaerobic CO_2 emission or mineralization of peat from previous studies

Nature of the peat	Depths of sampling (cm)	Q_{10}	Reference
Poor fen in France	5-10 cm (4-28°C)	1.90 ± 0.23	(Li et al., 2021)
	35-40 cm (4-28°C)	2.18 ± 0.32	
Plateau bog	0 cm (4-12°C)	1.09	(Waddington et al., 2001)
	0 cm (12-20°C)	1.77	
	5 cm (4-12°C)	1.12	
	5 cm(12-20°C)	1.68	
	10 cm (4-12°C)	1.15	
	10 cm(12-20°C)	1.92	
	75 cm (4-12°C)	2.33	
	75 cm (12-20°C)	2.43	
Boreal forest peatland	10 cm (4-15°C)	2.87	(McKenzie et al., 1998)
	10 cm (15-25°C)	1.69	
	25 cm (4-15°C)	2.37	
	25 cm (15-25°C)	1.92	
	25 cm (4-15°C)	2.37	
	25 cm (15-25°C)	1.92	
	50 cm (4-15°C)	2.85	
	50 cm (15-25°C)	3.40	
Moor House National Nature Reserve in UK	0-10 cm (5-15°C)	3.3	(Hardie et al., 2011)
	10-20 cm (5-15°C)	3.9	
	20-30 cm (5-15°C)	3.8	
Low moor peatland	0-20 cm (10-20°C)	2.44	(Szafranek-Nakonieczna and Stepniewska, 2014)
	20-40 cm (10-20°C)	1.68	
	40-60 cm (10-20°C)	1.73	
	60-80 cm (10-20°C)	4.54	
High peatlands	0-20 cm (10-20°C)	4.63	
	20-40 cm (10-20°C)	6.53	
	40-60 cm (10-20°C)	6.28	
	60-80 cm (10-20°C)	4.06	
Zoige peatland	0-10cm (8-18°C)	1.80	(Liu et al., 2019)
	11-20cm (8-18°C)	2.21	
	21-30cm (8-18°C)	1.57	
	31-40cm (8-18°C)	1.30	
	41-50cm (8-18°C)	1.69	
	51-60cm (8-18°C)	1.71	
	61-70cm (8-18°C)	2.16	

71-80cm (8-18°C)	2.02
81-90cm (8-18°C)	1.60
91-100cm (8-18°C)	1.25

References

Cole, J.J., Carpenter, S.R., Pace, M.L., Van De Bogert, M.C., Kitchell, J.L., Hodgson, J.R., 2006. Differential support of lake food webs by three types of terrestrial organic carbon. Ecol. Lett. 9, 558–568. https://doi.org/10.1111/j.1461-0248.2006.00898.x

Cory, R.M., McKnight, D.M., 2005. Fluorescence spectroscopy reveals ubiquitous presence of oxidized and reduced quinones in dissolved organic matter. Environ. Sci. Technol. 39, 8142–8149. https://doi.org/10.1021/es0506962

D'Andrilli, J., Junker, J.R., Smith, H.J., Scholl, E.A., Foreman, C.M., 2019. DOM composition alters ecosystem function during microbial processing of isolated sources. Biogeochemistry 142, 281–298. https://doi.org/10.1007/s10533-018-00534-5

Gao, Z., Guéguen, C., 2017. Size distribution of absorbing and fluorescing DOM in Beaufort Sea, Canada Basin. Deep. Res. Part I Oceanogr. Res. Pap. 121, 30–37. https://doi.org/10.1016/j.dsr.2016.12.014

Hardie, S.M.L., Garnett, M.H., Fallick, A.E., Rowland, A.P., Ostle, N.J., Flowers, T.H., 2011. Abiotic drivers and their interactive effect on the flux and carbon isotope (14C and δ13C) composition of peat-respired CO2. Soil Biol. Biochem. 43, 2432–2440. https://doi.org/10.1016/j.soilbio.2011.08.010

Li, Q., Leroy, F., Zocatelli, R., Gogo, S., Jacotot, A., Guimbaud, C., Laggoun-Défarge, F., 2021. Abiotic and biotic drivers of microbial respiration in peat and its sensitivity to temperature change. Soil Biol. Biochem. 153, 108077. https://doi.org/10.1016/j.soilbio.2020.108077

Liu, L., Chen, H., Jiang, L., Zhan, W., Hu, J., He, Y., Key, C.A.S., Ecological, M., Utilization, B., Restoration, E., Conservation, B., 2019. Response of anaerobic mineralization of different depths peat carbon to warming on Zoige plateau 337, 1218–1226. https://doi.org/10.1016/j.geoderma.2018.10.031

McKenzie, C., Schiff, S., Aravena, R., Kelly, C., St. Louis, V., 1998. Effect of temperature on production of CH4 and CO2 from peat in a natural and flooded boreal forest wetland. Clim. Change. https://doi.org/10.1023/A:1005416903368

Szafranek-Nakonieczna, A., Stepniewska, Z., 2014. Aerobic and anaerobic respiration in profiles of Polesie Lubelskie peatlands. Int. Agrophysics 28.

Tfaily, M.M., Corbett, J.E., Wilson, R., Chanton, J.P., Glaser, P.H., Cawley, K.M., Jaffé, R., Cooper, W.T., 2015. Utilization of PARAFAC-modeled excitation-emission matrix (EEM) fluorescence spectroscopy to identify biogeochemical processing of dissolved organic matter in a Northern peatland. Photochem. Photobiol. 91, 684–695. https://doi.org/10.1111/php.12448

Waddington, J.M., Rotenberg, P.A., Warren, F.J., 2001. Peat CO2 production in a natural and cutover peatland: Implications for restoration. Biogeochemistry 54, 115–130. https://doi.org/10.1023/A:1010617207537

Zhou, Y., Martin, P., Müller, M., 2019. Composition and cycling of dissolved organic matter from tropical peatlands of coastal Sarawak, Borneo, revealed by fluorescence spectroscopy and parallel factor analysis. Biogeosciences 16, 2733–2749. https://doi.org/10.5194/bg-16-2733-2019

Zhuang, W.E., Chen, W., Cheng, Q., Yang, L., 2021. Assessing the priming effect of dissolved organic

matter from typical sources using fluorescence EEMs-PARAFAC. Chemosphere 264, 128600. https://doi.org/10.1016/j.chemosphere.2020.128600